Journal of Medicinal Chemistry

Article

pubs.acs.org/jmc

Discovery of Coumarin−Dihydropyridine Hybrids as Bone Anabolic Agents

Koneni V. Sashidhara,*[,†] Manoj Kumar,[†,∥] Vikram Khedgikar,[‡,∥] Priyanka Kushwaha,[‡] Ram K. Modukuri,[†] Abdhesh Kumar,[†] Jyoti Gautam,[‡] Divya Singh,[‡] Balasubramaniam Sridhar,[§] and Ritu Trivedi*[,‡]

[†]Medicinal and Process Chemistry Division, CSIR-Central Drug Research Institute (CSIR-CDRI), Lucknow, 226 001, India

[‡]Endocrinology Division, CSIR-Central Drug Research Institute (CSIR-CDRI), Lucknow, 226 001, India

[§]Laboratory of X-ray Crystallography, CSIR-Indian Institute of Chemical Technology (CSIR-IICT), Hyderabad, 500 007, India

Supporting Information

ABSTRACT: The concept of molecular hybridization led us to discover a novel series of coumarin−dihydropyridine hybrids that have potent osteoblastic bone formation in vitro and that prevent ovariectomy-induced bone loss in vivo. In this context, among all the compounds screened for alkaline phosphatase activity, four compounds **10**, **14**, **18**, and **22** showed significant activity at picomolar concentrations. A series of other in vitro data strongly suggested compound **18** as the most promising bone anabolic agent, which was further evaluated for in vivo studies. From these studies compound **18** proved to be useful, which at low oral dose of 1 (mg/kg)/day body weight increased bone mass density and volume, expression of osteogenic genes (RUNX2, BMP-2, and ColI), bone formation rate (BFR), and mineral apposition rate (MAR), improved the trabecular microarchitecture, and decreased bone turn over markers in an ovariectomized rodent model for postmenopausal osteoporosis.

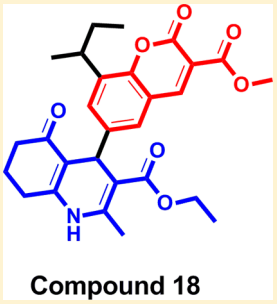

INTRODUCTION

Bone is a living, dynamic tissue that is constantly remodeled in the process of bone turnover. Bone health in adult life depends on the synchronized performance of bone forming osteoblasts and bone resorbing osteoclasts that function together on the bone surface.[1] An imbalance in the activities of bone resorbing osteoclast cells and bone-depositing osteoblast cells upon aging or menopause leads to osteoporosis.[2] It is the most common metabolic bone disorder, and over a lifetime, leads to skeletal fragility, which increases vulnerability to fractures due to the rapid loss of mineralized bone tissue and elevated rate of bone turnover.[3] Estrogen withdrawal after menopause in women physiologically alters the potential of mesenchymal stem cells (MSCs) of the bone marrow to differentiate more toward adipocytes and less to osteoblasts, disturbing bone formation and favoring bone resorption as revealed by numerous clinical studies and reports.[4] Increased adipogenesis in the bone marrow augments production of adipokines that stimulate osteoclast differentiation and functions.[5] As a result, these individuals are at risk for spontaneous, atraumatic (or mild trauma) fractures.

Besides osteoporosis, the aging population has an increasing threat of developing disorder, such as high blood pressure, that is linked to malfunctions in calcium metabolism and homeostasis leading to increased calcium loss.[6] High blood pressure triggers the parathyroid gland and augments removal of calcium from bone. Reports also suggest that compared to normotensive subjects, hypertensive patients have an increased urinary calcium excretion (hypercalciuria), which causes reduced bone mineral density.[7]

1,4-Dihydropyridines (Hantzsch ester), a well-known class of calcium channel antagonists, are most widely clinically used for more than decades. Recently Halici et al. reported that amlodipine, a dihydropyridine calcium channel blocker, increases calcium and phosphate concentrations in femur in ovariectomized rats.[8] In addition, Fujimura et al. have demonstrated protective effect of amlodipine against osteoporosis in stroke-prone hypertensive rats. Their study revealed that amlodipine might exert its effect through a direct inhibition of osteoclast function and/or suppression of parathyroid hormone secretion and subsequent inhibition of osteoclast activity.[9]

Coumarins, also known as benzopyran-2-ones, are a family of naturally occurring lactones and have attracted intense interest in recent years because of their diverse pharmacological properties.[10] Coumarins have also been extensively studied for their antiosteoporotic effects.[11] In the area of osteoporosis, there has been rising interest in bone anabolic agents that improve bone health. In the design of new drugs, the concept of molecular hybridization is an attractive strategy. It is based on the combination of two pharmacophoric moieties of different bioactive substances to produce a new hybrid compound that is more medically effective than its individual components. Our design concept was based on the molecular hybridization of coumarin and dihydropyridine subunits to produce fused novel hybrid derivatives containing dual pharmacophores (antihypertensive and antiosteoporotic) in a

Received: September 5, 2012
Published: December 5, 2012

dx.doi.org/10.1021/jm301281e | J. Med. Chem. 2013, 56, 109−122

Scheme 1. Synthesis of Coumarin−Dihydropyridine Hybrids[a]

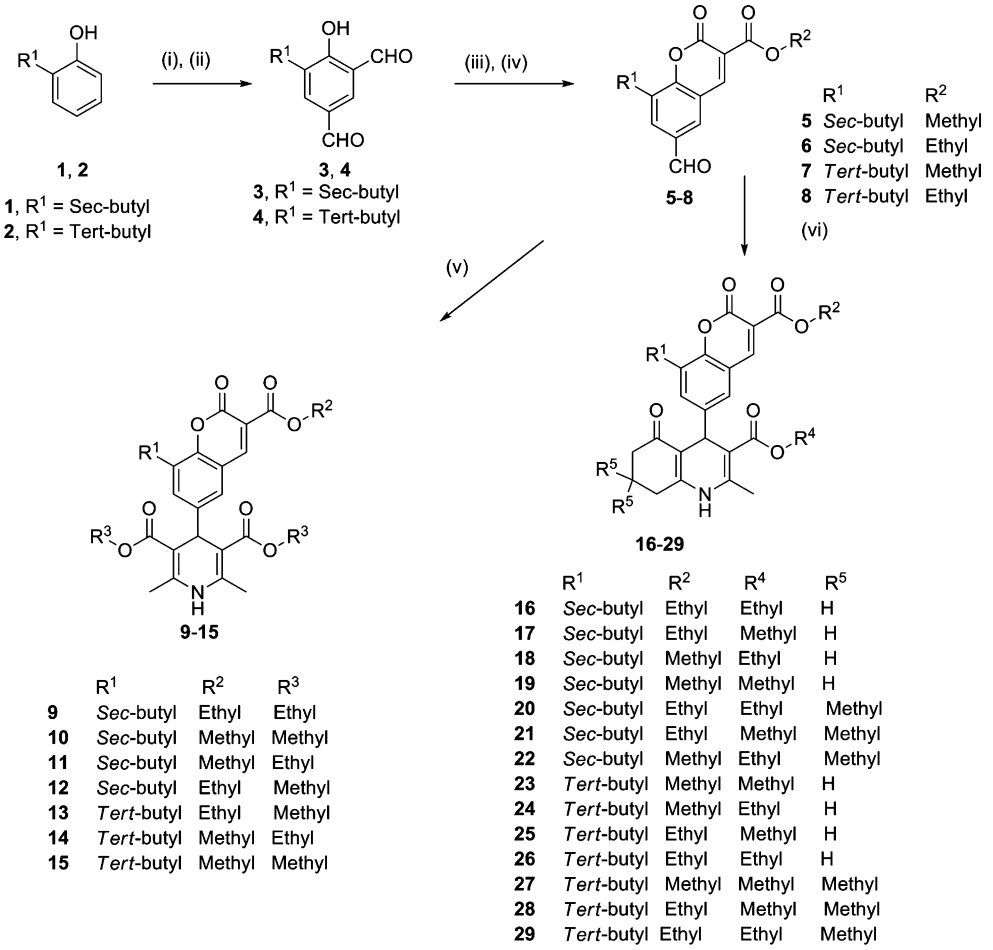

	R^1	R^2	R^3
9	*Sec*-butyl	Ethyl	Ethyl
10	*Sec*-butyl	Methyl	Methyl
11	*Sec*-butyl	Methyl	Ethyl
12	*Sec*-butyl	Ethyl	Methyl
13	*Tert*-butyl	Ethyl	Methyl
14	*Tert*-butyl	Methyl	Ethyl
15	*Tert*-butyl	Methyl	Methyl

	R^1	R^2	R^4	R^5
16	*Sec*-butyl	Ethyl	Ethyl	H
17	*Sec*-butyl	Ethyl	Methyl	H
18	*Sec*-butyl	Methyl	Ethyl	H
19	*Sec*-butyl	Methyl	Methyl	H
20	*Sec*-butyl	Ethyl	Ethyl	Methyl
21	*Sec*-butyl	Ethyl	Methyl	Methyl
22	*Sec*-butyl	Methyl	Ethyl	Methyl
23	*Tert*-butyl	Methyl	Methyl	H
24	*Tert*-butyl	Methyl	Ethyl	H
25	*Tert*-butyl	Ethyl	Methyl	H
26	*Tert*-butyl	Ethyl	Ethyl	H
27	*Tert*-butyl	Methyl	Methyl	Methyl
28	*Tert*-butyl	Ethyl	Methyl	Methyl
29	*Tert*-butyl	Ethyl	Ethyl	Methyl

[a]Reagents and conditions: (i) HMTA, TFA, 120 °C, 4 h; (ii) aq H_2SO_4, 100 °C, 2 h; (iii) diethyl/methyl malonate, EtOH, piperidine, reflux, 30 min; (iv) glacial AcOH, rt; (v) ethyl/methyl acetoacetate, NH_4OAc, AcOH, EtOH, reflux, 5 h; (vi) ethyl/methyl acetoacetate, dimedone, NH_4OAc, AcOH, EtOH, reflux, 5 h.

single structure. Motivated by the hybrid approach and our own interest in this class of compounds,[12] we report here the design and synthesis of coumarin−dihydropyridine hybrids for the treatment of postmenopausal osteoporosis in ovariectomized rodent model.

CHEMISTRY

The synthetic routes followed for the preparation of the coumarin derivatives and coumarin−dihydropyridines hybrids are illustrated in Scheme 1. The Duff formylation reaction on *o*-alkyl substituted phenols (**1**, **2**) in the presence of hexamethylenetetramine (HMTA) and trifluoracetic acid (TFA) followed by hydrolysis using 10% aqueous H_2SO_4 solution gave the dicarbaldehyde intermediates (**3**, **4**). These dialdehyde intermediates were then engaged in the Knoevenagel-type reaction with different active methylene compounds resulting in the formation of coumarinic compounds (**5**−**8**).[13] Further, these coumarinic aldehyde compounds were subjected to Hantzsch-type cyclocondensation reaction, involving coumarinic aldehydes (**5**−**8**), active methylene compounds, and ammonium acetate (nitrogen donor).[14] For symmetrical Hantzsch dihydropyridines (**9**−**15**), an amount of 2 equiv of ethyl/methyl acetoacetate was used, while for unsymmetrical Hantzsch polyhydroquinolines (**16**−**29**), uniequivalent of ethyl/methyl acetoacetate and substituted 1,3-cyclic diketones were used. Initially, various acidic catalysts such as boric acid, camphor sulfonic acid, sodium dodecyl sulfate (SDS), *p*-toluenesulfonic acid (*p*TSA), and glacial acetic acid were screened for the synthesis. However, glacial acetic acid was found to be the best among all the catalysts used. Although the reaction was slow in various solvents, ethanol was found to be the best among all the solvents used for the reaction.

All the final compounds (**9**−**29**) as well as intermediates (**5**−**8**) were afforded in excellent yields. All compounds were characterized using ^{1}H NMR, ^{13}C NMR, 2D NMR, mass spectrometry, and IR spectroscopy. Additionally, the structure of a representative compound **15** (Figure 1) was unambiguously confirmed by single crystal X-ray analysis (CCDC number 877578; refer to the Supporting Information for details).

RESULTS AND DISCUSSION

Preliminary Screening of Coumarin−Dihydropyridine Hybrids Using Osteoblast Differentiation Assay. Coumarin intermediates (**5**−**8**) and final hybrid compounds (**9**−**29**) were screened for alkaline phosphatase (ALP, a marker of osteoblast differentiation) activity in primary calvarial osteoblasts. Cells were treated with synthesized compounds and evaluated for ALP activity at concentrations ranging from 1 pM to 1 μM. ALP activity was assessed spectrophotometrically, and

dx.doi.org/10.1021/jm301281e | *J. Med. Chem.* 2013, 56, 109−122

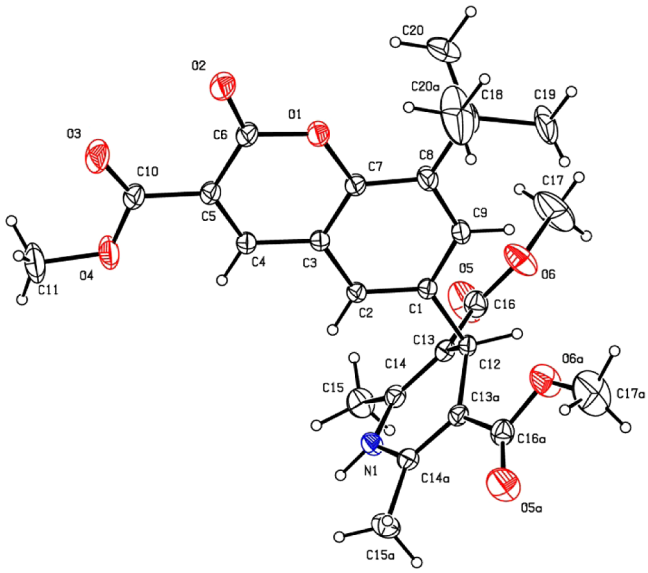

Figure 1. X-ray crystallographic structure of compound **15**.

optical density was measured at 405 nm. Table 1 shows the % ALP activity together with EC_{50} and E_{max} values for all the synthesized compounds. Though most hybrids significantly stimulated ALP activity in osteoblasts, suggesting increased osteoblast differentiation, two active compounds from each structural class represented by **10** and **14** (symmetrical hybrids) and compounds **18** and **22** (unsymmetrical hybrids) were chosen for subsequent work. Nifedipine exhibited ALP activity at 10 nM, while our synthesized hybrids showed activity at much lower concentrations (picomolar concentrations). Compounds **10** and **18** exhibited significant activity at as low as 1 and 100 pM, respectively (Figure 2). This experiment noticeably demonstrated that coumarin−dihydropyridine hybrids were found to be more potent than individual coumarins (**5**−**8**) or nifedipine.[15]

Table 1. Alkaline Phosphatase Activity of Synthesized Hybrids[a]

compd	E_{max}	EC_{50} (μM)	ALP activity (%)	ALP activity (%) compared with nifedipine
nifedipine	10 nM	1.45	25 ($p < 0.01$)	
5			inactive	
6	10 nM	1.49	6	NS
7			inactive	
8			inactive	
9	100 pM	1.23	4	NS
10	1 pM	1.19	30 ($p < 0.01$)	12 ($p < 0.05$)
11	100 pM	1.14	5	NS
12	10 nM	1.51	20 ($p < 0.01$)	NS
13	1 pM	1.04	7	NS
14	100 pM	1.10	70 ($p < 0.001$)	28 ($p < 0.001$)
15			Inactive	
16	1 pM	1.01	35 ($p < 0.01$)	14 ($p < 0.05$)
17	100 pM	1.23	12	NS
18	100 pM	1.17	80 ($p < 0.001$)	32 ($p < 0.001$)
19	10 nM	1.56	4	NS
20	100 pM	1.28	3	NS
21	1 pM	1.19	39 ($p < 0.01$)	16 ($p < 0.05$)
22	1 pM	1.01	43 ($p < 0.001$)	17 ($p < 0.05$)
23	100 pM	1.34	14 ($p < 0.05$)	NS
24	1 pM	1.26	4	NS
25	1 pM	1.31	10	NS
26	1 pM	1.34	13 ($p < 0.05$)	
27	10 nM	1.53	10	NS
28	1 pM	1.09	5	
29	10 nM	1.56	4	NS

[a]NS: not significant.

Coumarin−Dihydropyridine Hybrids Show No Toxicity on Osteoblasts within the Effective Concentrations. The toxicity of these four active compounds was tested on calvarial osteoblast cells.[16] Apparently, these compounds when assessed for percent proliferation showed no toxicity to osteoblast cells compared to the control group at doses ranging from 1 pM to 1 μM (Figure 3). All the compounds **10**, **14**, **18**, and **22** showed significant proliferation of osteoblastic cells at concentrations that were comparable to that of nifidipine, which is a clinically approved drug for treatment of hypertension.

Mineralization Ability of Active Compounds in Calvarial Osteoblast Cells. Compounds that were found active for ALP activity (**10**, **14**, **18**, and **22**) were further evaluated for their osteogenic activity by mineralization assay. Calvarial osteoblast cells at the end of the differentiation process with or without treatment with the compounds for 21 days were fixed and stained with alizarin red-S. Alizarin red-S stains the newly formed mineralized nodules that deposit calcium. Compounds **10**, **14**, **18**, and **22** showed significantly increased mineralizing ability compared to the control untreated cells. Quantification of mineralization by optical density measurement of alizarin red-S extracted from stained cultures showed significant increase in mineralization of osteoblasts cultured in the presence of these compounds. Table 2 shows the EC_{50} and E_{max} values of mineralization for all the active compounds. Data suggest that compound **18** (at 100 pM) was found to be the most potent ($P < 0.001$ vs corresponding control group) and showed approximately 65−70% increased mineralization compared to control untreated cells and standard compound nifidipine. This was followed by activity of compounds **10**, **14**, and **22** whose activity was comparable to that of nifidipine but was less than that of compound **18** (Figure 4).[15]

Active Compounds Increase Osteoblastogenesis Related Marker Gene Expressions. We next studied the effect of active compounds (**10**, **14**, **18**, and **22**) on the expression of various osteogenic genes including Runx-2, BMP-2, alkaline phosphatase (ALP), osteocalcin (OCN), and type I collagen (ColI) in calvarial osteoblast cells by qPCR (Figure 5). The housekeeping gene GAPDH was used as the internal control in this study.

Runx-2, a bone-specific transcription factor, is a key regulator of osteoblast differentiation and is important for expression of ALP and collagen I (biomarker of osteoblast differentiation).[17] Furthermore, we also studied the effect of potent hybrids on the relative expression of bone morphogenetic protein (BMP-2) that is estrogenic regulated gene involved in bone differentiation. The transcript levels of Runx-2, ALP, ColI, BMP-2, and OCN were assessed by qPCR after treatment with compounds, and results were expressed as fold change over untreated cells. Our data show that expression of osteogenic genes after treatment with compounds increased from ∼1.5- to ∼3.0-fold, with maximum increase being with compound **18** at 100 pM. Interestingly, the unsymmetrical hybrids (compounds

dx.doi.org/10.1021/jm301281e | J. Med. Chem. 2013, 56, 109−122

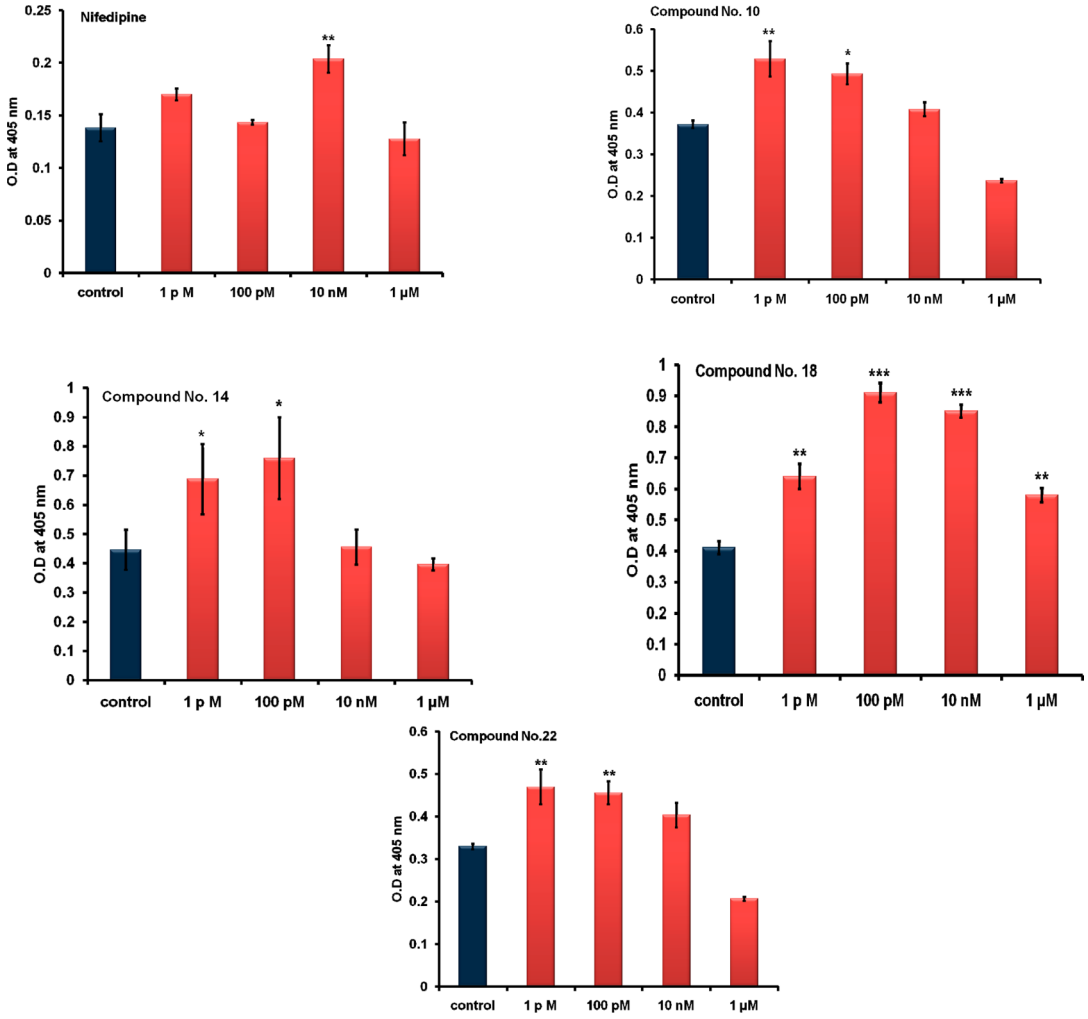

Figure 2. Activity of the potent hybrids at various concentrations as assessed by alkaline phosphatise (ALP) activity in calvarial osteoblast cells. At the end of the experiment, ALP activity was measured colorimetrically. Data represent the mean ± SEM from three independent experiments: (***) $p < 0.001$, (**) $p < 0.01$, and (*) $p < 0.05$ compared with untreated cells taken as control.

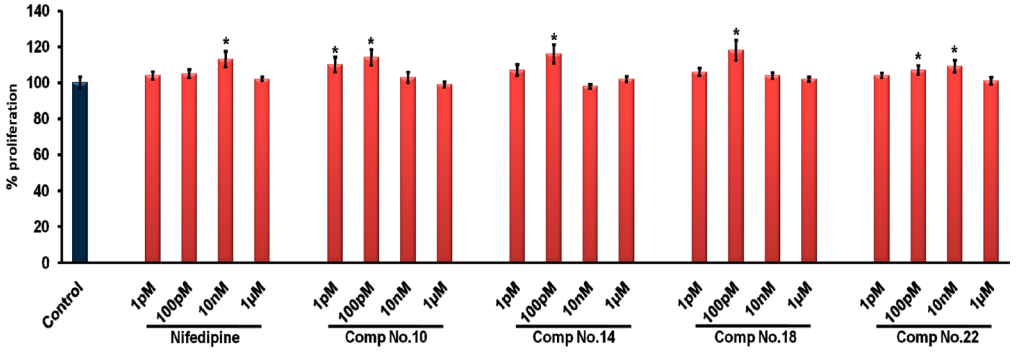

Figure 3. Active hybrids increase cell proliferation of calvarial osteoblast cells. Cells were cultured in differentiation medium and treated with various concentrations of the compound ranging from 1 pM to1 μM for 48 h, and cell viability was assessed by MTT assay. The percent viable cells was calculated compared to untreated cells taken as control. Data represent the mean ± SEM from three independent experiments.

Table 2. E_{max} and EC_{50} of Active Hybrids for Mineralization

	nifedipine	**10**	**14**	**18**	**22**
E_{max}	10 nM	1 pM	100 pM	100 pM	100 pM
EC_{50} (μM)	1.54	1.01	1.14	1.23	1.17

18 and **22**) exhibited significant expression of various osteogenic genes compared with the symmetrical hybrids (compounds **10** and **14**). The expression pattern of various important genes (BMP-2, RunX2, and ColI) was also substantiated by Western blot analysis to confirm the corresponding changes in the protein levels for target proteins (Figure 6). Thus, taken together, active compounds increase differentiation and mineralization of osteogenic genes in calvarial osteoblast cells in the following order: compound **18** > compound **14** > compound **22** > compound **10**.[18] Together,

dx.doi.org/10.1021/jm301281e | J. Med. Chem. 2013, 56, 109−122

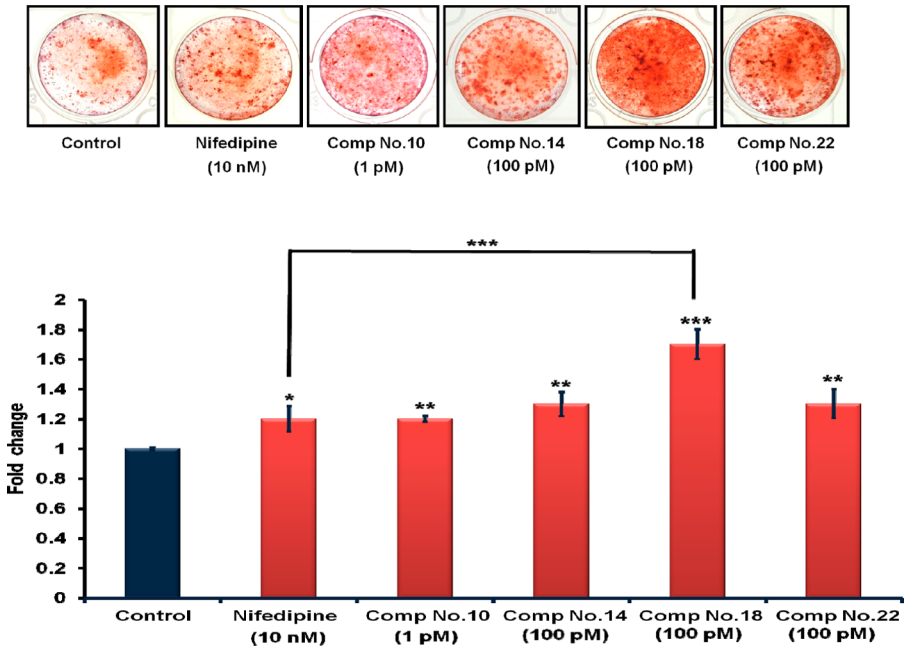

Figure 4. Calvarial osteoblasts cells were grown in osteoblast differentiation medium. Cultures were maintained for 21 days. At the end of the experiments, cells were stained with alizarin red-S. Top: Representative photomicrographs showing mineralized nodules in various groups with or without treatment. Bottom: Alizarin red-S dye was extracted and mineralization quantified spectrophotometrically. Data are represented as the mean ± SEM from three independent experiments ((∗) $p < 0.05$, (∗∗) $p < 0.01$, and (∗∗∗) $p < 0.001$ compared to control).

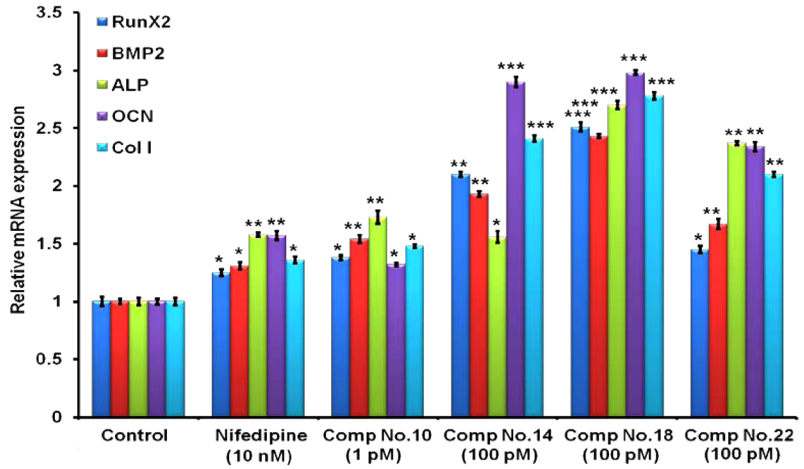

Figure 5. qPCR analysis showing increase in mRNA expression of osteogenic marker genes. RunX-2, BMP-2, collagen I (Col I), alkaline phosphatase (ALP), and osteocalcin (OCN) have been treated with compounds **10**, **14**, **18**, and **22** compared with nifedipine in calvarial osteoblast cells. qPCR data of the indicated genes represent the mean ± SEM from three independent experiments.

our results demonstrated that compound **18** significantly increased alkaline phosphatase activity, mineralization, and the expression of various key osteogenic genes. Therefore, we took compound **18** for further detailed in vivo evaluation in ovariectomized mice.

Detailed in Vivo Evaluation of the Lead. Lead Compound 18 Treatment Improves Trabecular Microarchitecture in OVx Mice. Trabecular bone is easily lost in the OVx condition; hence, it was of interest to study if compound **18** is able to protect against the deterioration of trabecular microarchitecture as a result of OVx. Figure 7 shows representative images of tibial metaphysic reconstructed 3D μCT images of trabecular microarchitecture among the various treatment groups. It is evident from the images that when compared with the sham group, the OVx group had significantly deteriorated bone microarchitecture. Treatment with compound **18** significantly restored the microarchitecture at all doses (1, 5, 10 (mg/kg)/day) with improved bone parameters.[19−22] Table 3 summarizes the microarchitectural parameters of bone as assessed by μCT.[29−31] Ovariectomy is typically associated with reduction in trabecular separation, numbers, connectivity, and platelike structures. Data reveal that ovariectomy resulted in significant microarchitectural deteriorations indicated by reduced bone volume/trabecular volume (BV/TV), trabecular number (Tb.N), together with increased trabecular separation (Tb.Sp) and structural model index (SMI). SMI is used to assess "platelike" trabeculae. Higher SMI indicates deterioration of trabeculae from platelike to "rodlike" structure. The treatment of compound **18** for 8 weeks to OVx mice restored the microarchitectural parameters in a dose

dx.doi.org/10.1021/jm301281e | J. Med. Chem. 2013, 56, 109−122

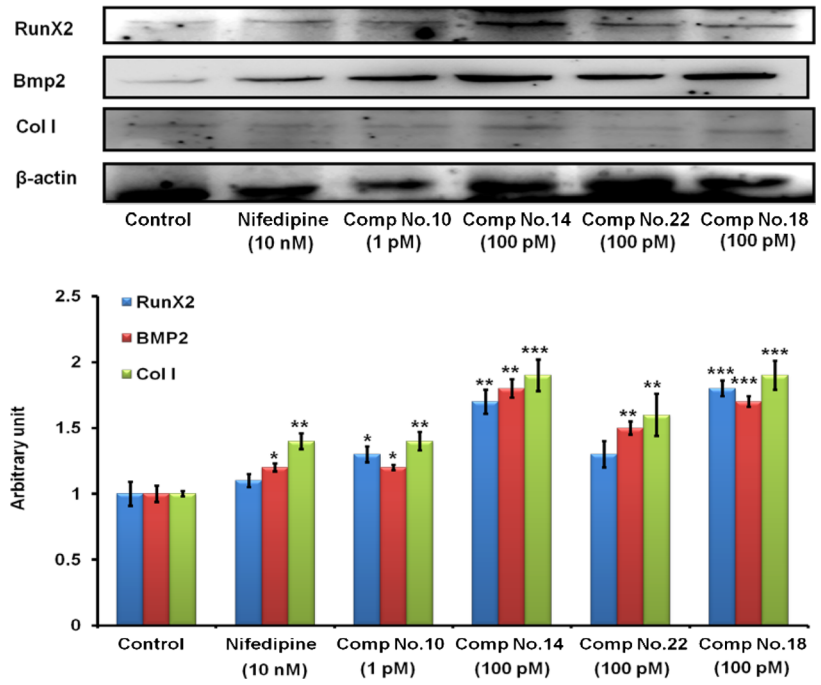

Figure 6. Western blot of BMP-2, RunX2, and Col I. Osteoblasts were treated with or without various compounds for 48 h. Proteins extracted from cell lysates were transblotted onto a membrane and probed with primary antibodies followed by the corresponding secondary antibodies normalized with β-actin. Graph shows the densitometric analysis (fold change) of the observed change in expression of the proteins.

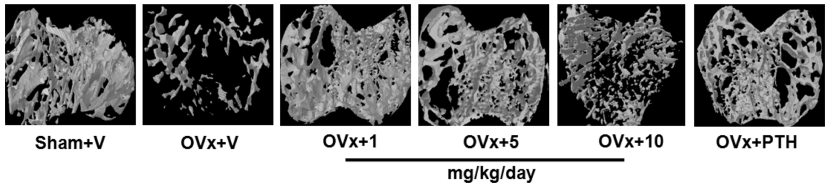

Figure 7. Restoration of bone microarchitectural parameters by treatment with compound **18**. Figure shows representative μCT image of the cross-section of the tibial proximal region. Treatment of compound **18** to OVx mice improved trabecular microarchitecture, as is clearly visible when compared with OVx mice.

Table 3. Microarchitectural Parameters of Tibia[a]

trabecular parameters of tibial metaphysis	sham + vehicle	OVx + vehicle	OVx + 1 (mg/kg)/day	OVx + 5 (mg/kg)/day	OVx + 10 (mg/kg)/day	OVx + PTH
BV/TV (%)	3.61 ± 0.17***	0.45 ± 0.07	2.85 ± 0.05***	2.33 ± 0.16***	2.07 ± 0.23***	2.85 ± 0.45***
Tb.Sp (mm)	0.65 ± 0.01***	0.99 ± 0.08	0.66 ± 0.02***	0.72 ± 0.03***	0.68 ± 0.02***	0.61 ± 0.03***
Tb.N (mm^{-1})	0.47 ± 0.34***	0.12 ± 0.02	0.40 ± 0.03***	0.30 ± 0.03***	0.32 ± 0.01***	0.42 ± 0.06***
SMI	2.08 ± 0.05***	2.68 ± 0.05	2.32 ± 0.05**	2.31 ± 0.05**	2.19 ± 0.06***	2.44 ± 0.11*

[a]Each parameter represents pooled data from 10 mice/group, and values are expressed as the mean ± SE: (***) $p < 0.001$, (**) $p < 0.01$, and (*) $p < 0.05$ compared with OVx + vehicle group. Interdose comparison of compound **18** shows that for 1 (mg/kg)/day dose $P < 0.01$, $P < 0.05$ when compared with OVx + 5 (mg/kg)/day group and $p < 0.01$, $p < 0.05$ when compared with OVx + 10 (mg/kg)/day group. $p < 0.01$ when OVx + 5 (mg/kg)/day compared with OVx + 10 (mg/kg)/day.

dependent manner, suggesting its potent bone restoring action. Compound **18** at a dose of 1 mg/kg increased BV/TV ($p < 0.001$) and Tb.N ($P < 0.001$) and decreased Tb.Sp. ($P < 0.001$) and SMI ($P < 0.05$). Similar to 1 (mg/kg)/day dose, doses of 5 and 10 (mg/kg)/day body weight also restored the bone microarchitectural parameters. Interdose comparison shows that the lower dose of 1 (mg/kg)/day exhibited the best response and was comparable to standard bone anabolic agent PTH which improved trabecular microarchitecture parameter BV/TV ($p < 0.001$) and Tb.N ($p < 0.001$) and decreased SMI ($p < 0.05$) which were comparable to sham control animals.

Lead Compound 18 Treatment Reduces Bone Turnover Markers Due to Ovariectomy. Ovariectomy induced bone loss is characterized by higher bone turnover rates, i.e., increase in both bone formation and resorption. As expected, the bone turnover markers (serum osteocalcin and CTx) levels are elevated in the OVx + V group compared with sham + V group (Figure 8). Treatment with compound **18** to OVx mice significantly lowered the levels of these markers, indicating attenuation of bone turnover and resorption.

The serum osteocalcin levels of OVx mice treated with 1.0 and 5.0 mg/kg compound **18** were comparable to that of the sham + vehicle group (Figure 8A), while the CTx serum levels

dx.doi.org/10.1021/jm301281e | J. Med. Chem. 2013, 56, 109−122

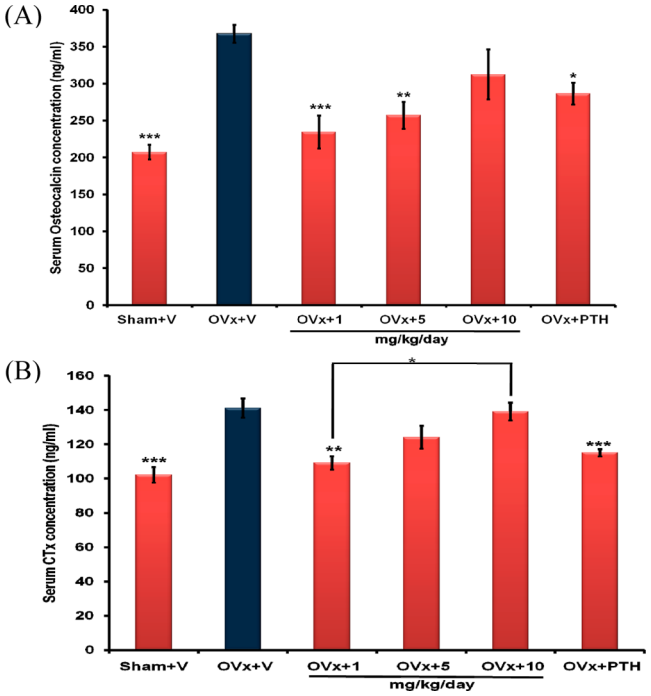

Figure 8. Compound **18** is effective in reducing bone turnover markers in OVx mice. (A) Serum osteocalcin levels and (B) serum CTx levels were significantly reduced in OVx mice treated with dose (1 and 5 mg/kg/dose in the case of osteocalcin and 1 (mg/kg)/day in CTx) compared with OVx + vehicle group. n = 10 mice/group were used for serum samples assayed in duplicate. Data represent the mean ± SEM: (***) $P < 0.001$, (**) $P < 0.01$ compared with OVx + vehicle group.

were significantly reduced at 1 (mg/kg)/day dose of compound **18** and the levels were not different when compared with PTH and sham + V groups (Figure 8B). Overall data suggest that compound **18** could inhibit ovariectomy induced bone turnover rate that is characteristically increased under estrogen deficiency.[15]

Direct Effect of Lead Compound 18 on Bones of Ovariectomized Mice. As BMP-2 plays an important role in osteoblast differentiation and since coumarins have been found to be potent BMP-2 up-regulating agents,[11] we also studied expression of this gene using our compound **18**. Femoral bones from OVx + vehicle mice exhibited increased mRNA levels of osteoblast-specific genes including those for RUNX2, BMP-2, and type I collagen compared with the sham group ($P < 0.05$) (Figure 9). Compound **18** treatment to OVx mice resulted in a dose-dependent increase in the mRNA levels of all key genes. At 1 (mg/kg)/day compound **18** increased the expression of these osteogenic genes which was comparable with that of PTH treatment and significantly higher than that of the sham group.[23]

Effect of Compound 18 on Osteoclastic Gene Expression in Bones of Ovariectomized Mice. Since ovariectomy results in increased osteoclastogenesis, we determined the expression of osteoclast specific genes that includes TRAP (osteoclast differentiation marker) and RANK (osteoclast expression marker) as shown in Figure 10. Ovariectomy results in increased mRNA levels (25−45%) of these genes, demonstrating significantly high osteoclastic activity, $p < 0.001$ vs sham + V group and PTH treated group. Treatment with compound **18** restored the lost bone by attenuating the expression of TRAP and RANK genes with a dose of 1 mg/kg body weight being the most significant dose compared with 5 and 10 (mg/kg)/day ($p < 0.001$ and $p < 0.05$). Data were comparable to those of standard control PTH.

During bone remodeling, osteoblasts produce important paracrine signals that promote osteoclastogenesis. Reduction in OPG and increase in RANKL in OVx bones favor osteoclast differentiation and activation and promote bone loss. OPG and RANKL produced by osteoblasts regulate osteoclastogenesis and osteoclast function. We next studied whether or not compound **18** modulates osteoblast function such that osteoclastogenesis is inhibited. When data were expressed as a ratio of OPG/RANKL (measure of induction of osteoclastogenesis), compound **18** treatment of cocultures resulted in ∼6.0- to 8.0-fold increase in ratio. In the case of ovariectomized mice the OPG/RANKL ratio of 50% reduction was observed compared with the sham group ($p < 0.05$). The treatment with compound **18** increased the OPG/RANKL ratio; however, 1 (mg/kg)/day dose showed significant change when compared with 5 (mg/kg)/day dose ($p < 0.001$) and 10 (mg/kg)/day ($p < 0.001$).

Lead Compound 18 Initiates New Bone Formation in OVx Mice. To further validate the bone anabolic effect of compound **18**, we measured the parameters of new bone formation, i.e., mineral apposition rate (MAR) ($p < 0.001$) and bone formation rate (BFR) ($p < 0.001$), by dynamic histomorphometry in the femur bone (Figure 11). As was expected, the parameters of new bone formation were reduced in OVx mice compared with the sham group, as assessed by bone histomorphometry (Table 4). Compound **18** at doses 1, 5, and 10 mg/kg exhibited increase in BFR and MAR ($p < 0.001$) compared with OVx. The bone formation parameters were comparable to treatment with known bone anabolic agent PTH ($P < 0.001$). Statistical analysis of the data shows that 1 (mg/kg)/day dose showed the best response with MAR and BFR compared to the other two doses of 5 and 10 (mg/kg)/day. Comparison of BFR of 1 (mg/kg)/day dose with PTH showed significantly better response at the lower dose of compound **18**.

Effect of Compound 18 on in Vivo Toxicity and Liver Histomorphology. Finally, for preliminary safety evaluation of the lead compound, mice were treated with 1, 5, and 10 (mg/kg)/day compound **18** for 2 months orally. Livers from mice were harvested, and a histological examination was performed using a 5 μm thick section. The liver histomorphology of the treated and untreated animals was similar, and no morphological changes were observed (Figure 12). This preliminary study suggested that compound **18** would be safer for use in postmenopausal osteoporosis.

■ CONCLUSION

A novel series of coumarin−dihydropyridine hybrids was screened in estrogen deficiency model for osteoporosis in female Balb/c mice. In vitro data suggested compound **18** as most promising agent, which was further evaluated for in vivo studies using OVx mice model. Overall, the data indicate that in comparison to OVx mice (after estrogen withdrawal) treated with vehicle, compound **18** was nontoxic and at a lower dose of 1 (mg/kg)/day to OVx mice resulted in improved trabecular microarchitecture of the long bones, decreased bone turnover markers (osteocalcin and CTx), increased the expression of skeletal osteogenic genes (BMP-2 and RUNX-2), and increased new bone formation. The presence of compound **18** also

dx.doi.org/10.1021/jm301281e | J. Med. Chem. 2013, 56, 109−122

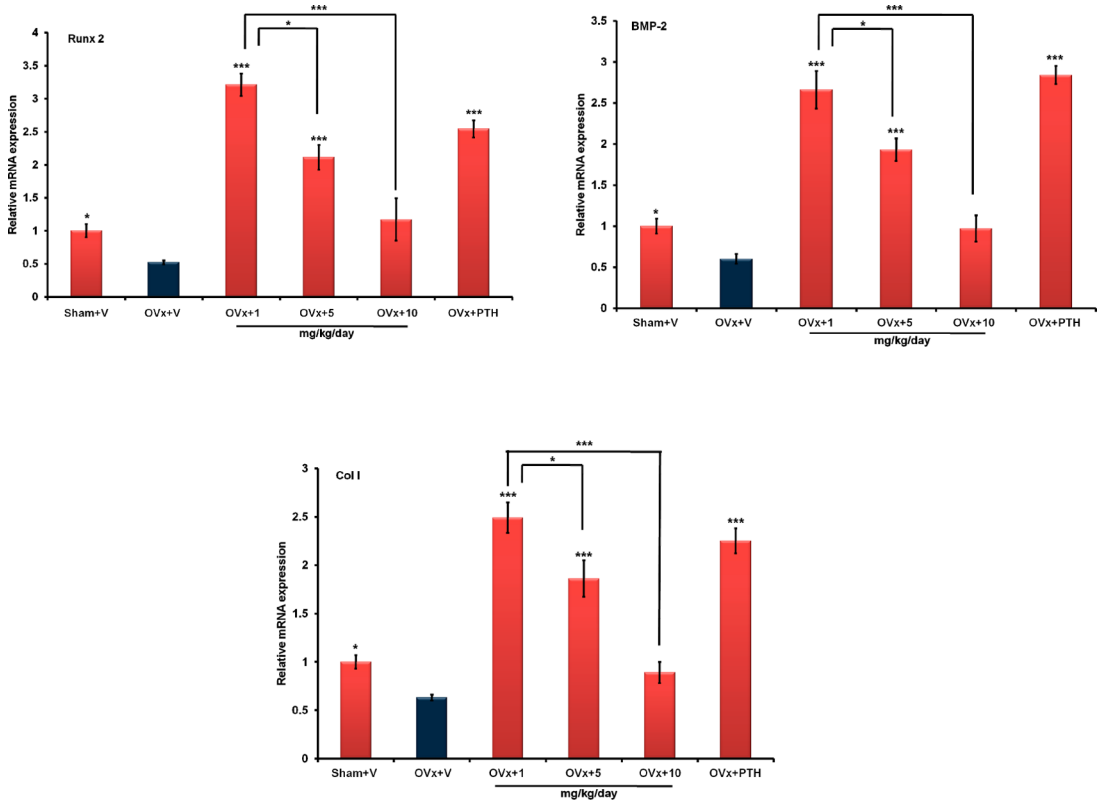

Figure 9. Compound **18** treatment to OVx mice increased various osteogenic genes. Total RNA was isolated from femur, and qPCR was performed to determine the mRNA levels of Runx-2, BMP-2, and type I collagen (Col1), and data were expressed after normalizing with GAPDH. Data represent the mean ± SEM, $n = 6$: (∗) $P < 0.05$, (∗∗∗) $P < 0.001$ compared with OVx mice bone.

increased osteoprotegrin (OPG/receptor activator of NFkB ligand (RANKL) ratio and reduced mRNA expression levels of osteoclast marker genes TRAP and RANK. Our findings point toward the direct inhibitory effect of compound **18** on osteoclastogenesis, thus contributing to bone sparing effect in ovariectomized mice. In vivo toxicity data show that compound **18** did not exhibit toxicity after oral administration. The exquisite potency and structural novelty of **18** suggest that it may serve as a valuable lead in the development of new class of bone anabolic agents. Thus, our findings clearly demonstrate the osteoprotective effects of compound **18** that was comparable to the known osteogenic agent, parathyroid hormone PTH. PTH is the only anabolic agent available for clinical use with parenteral route of administration and the risk of developing osteogenic sarcoma being major drawbacks associated with it. Being orally efficacious, compound **18** could be an attractive therapeutic option for the treatment of postmenopausal osteoporosis; however, more studies need to be done to position this compound for preclinical studies.

■ EXPERIMENTAL SECTION

General. All reagents were commercial and were used without further purification. Chromatography was carried on silica gel (60–120 and 100–200 mesh). All reactions were monitored by thin-layer chromatography (TLC). Silica gel plates with fluorescence F254 were used. Melting points were taken in open capillaries on a Complab melting point apparatus and are presented uncorrected. Infrared spectra were recorded on a Perkin-Elmer FT-IR RXI spectrophotometer. ^{1}H NMR and ^{13}C NMR spectra were recorded using BrukerSupercon magnet DRX-300 spectrometer (operating at 300 MHz for ^{1}H and 75 MHz for ^{13}C) using $CDCl_3$ as solvent and tetramethylsilane (TMS) as internal standard. Chemical shifts are reported in parts per million. Electrospray ionization mass spectra were recorded on a Thermo Lcq Advantage Max-IT instrument. High resolution mass spectra were recorded on 6520 Agilent Q Tof LC–MS/MS (accurate mass). Elemental analyses were performed on a Vario EL-III C, H, N, S analyzer (Germany) and Carlo-Erba-1108 C, H, N elemental analyzer (Italy), and values were within ±0.5% of the calculated values; therefore, these compounds meet the criteria of ≥95% purity.

General Synthesis of Compounds 3 and 4. *Synthesis of 5-sec-Butyl-4-hydroxybenzene-1,3-dicarbaldehyde (**3**).* 2-*sec*-Butylphenol **1** (5 g, 33.3 mmol) and hexamethylenetetramine (9.32 g, 66.6 mmol) were dissolved in TFA (25 mL), and the solution was heated at 120 °C for 4 h. After the mixture was cooled to room temperature, 10% aqueous H_2SO_4 (25 mL) was added and again the temperature was maintained at 90–100 °C for an additional 2 h. The solution was basified with Na_2CO_3 to pH 8 and extracted 3-fold with 50 mL of $CHCl_3$. The combined organic layers were dried on Na_2SO_4, filtered, and concentrated to dryness under reduced pressure. The crude products were purified over column chromatography (60–120 mesh) to afford (3.82 g, 55% yield) of compound **3** (5-*sec*-butyl-4-hydroxybenzene-1,3-dicarbaldehyde) as an oily liquid.

*5-sec-Butyl-4-hydroxybenzene-1,3-dicarbaldehyde (**3**).* Oily. Yield 55%. IR (neat): 3267, 2862, 1709, 1622, 1018 cm^{-1}. ^{1}H NMR ($CDCl_3$, 200 MHz) δ: 11.99 (s, 1H), 10.05 (s, 1H), 9.97 (s, 1H), 8.09 (brs, 1H), 8.01 (brs, 1H), 3.27–3.10 (m, 1H), 1.74–1.57 (m, 2H), 1.26 (d, 3H, J = 7.0 Hz), 0.86 (t, 3H, J = 7.3 Hz). ESI-MS m/z: 207 $(M + H)^+$.

*5-tert-Butyl-4-hydroxyisophthalaldehyde (**4**).* Oily. Yield 60%. IR (neat): 3262, 2865, 1703, 1626, 1013 cm^{-1}. ^{1}H NMR ($CDCl_3$, 300 MHz) δ: 12.39 (s, 1H), 9.99 (s, 1H), 9.93 (s, 1H), 8.07 (brs, 1H), 7.99 (brs, 1H), 1.46 (s, 9H). ESI-MS m/z: 207 $(M + H)^+$.

General Synthesis of Compounds 5–8. *Methyl 8-sec-Butyl-6-formyl-2-oxo-2H-chromene-3-carboxylate (**5**).* A solution of 5-*sec*-butyl-4-hydroxyisophthalaldehyde (0.5 g, 2.42 mmol) and dimethyl malonate (0.32 g, 2.42 mmol) in methanol (25 mL) was treated with

dx.doi.org/10.1021/jm301281e | J. Med. Chem. 2013, 56, 109–122

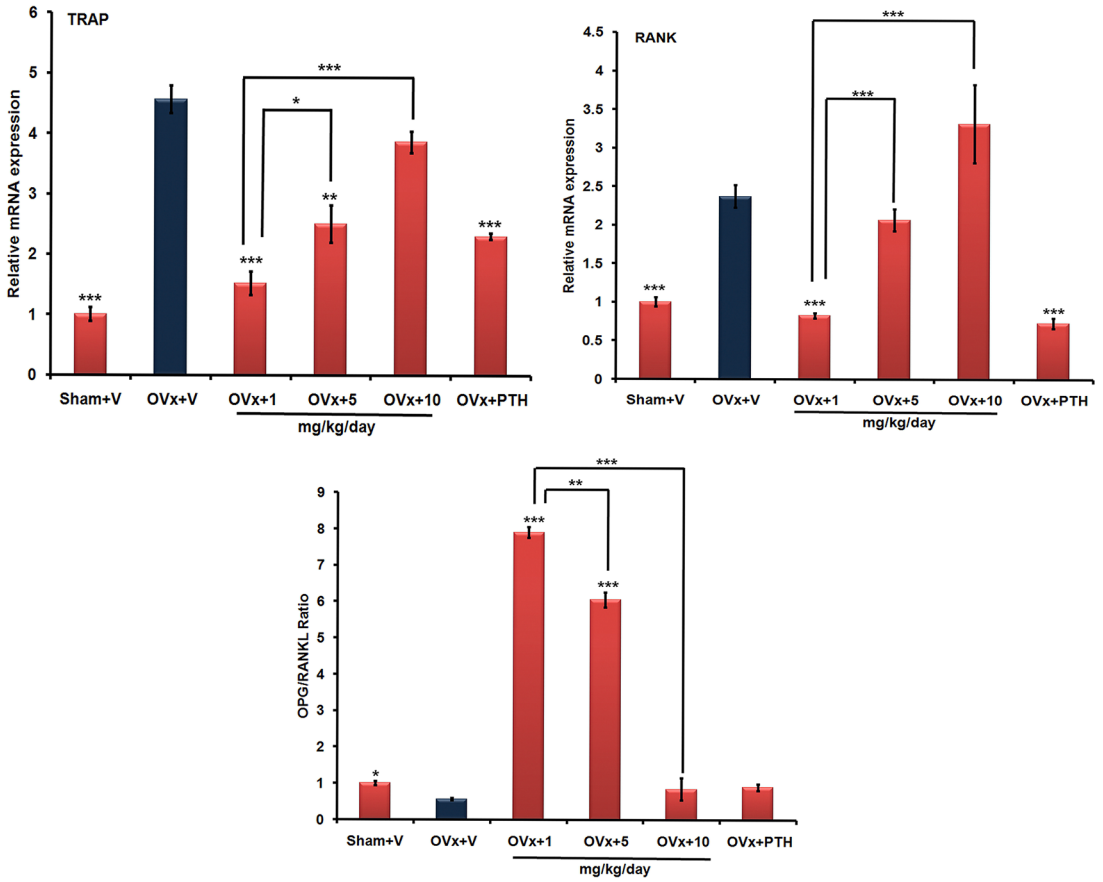

Figure 10. Compound **18** treatment suppresses the expression of osteoclastogenic genes in the long bones of ovariectomized mice. Total RNA was isolated from the long bones of various experimental groups. qPCR was performed to determine the m RNA levels of TRAP and RANK and OPG/RANKL ratio. Data are expressed after normalizing results with GAPDH. Data represent the mean ± SEM, $n = 6$: (∗) $P < 0.05$, (∗∗) $P < 0.01$, and (∗∗∗) $P < 0.001$ compared with OVx control group.

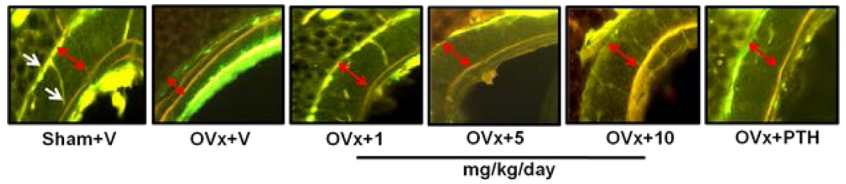

Figure 11. Compound **18** treatments promote new bone formation in mice. Representative images of transverse sections of tetracycline and calcein-labeled femur diaphyses from mice. After 8 weeks of treatment with vehicle or compound **18** (1, 5, and 10 (mg/kg)/day), tetracycline (UV filter) and calcein (orange) labeling are shown. Data are of 10 animals per group.

Table 4. Histomorphometric Parameters of Femur Bone from Compound 18 and Parathyroid Hormone Treated OVx Mice[a]

parameters	sham + vehicle	OVx + vehicle	OVx + 1 (mg/kg)/day	OVx + 5 (mg/kg)/day	OVx + 10 (mg/kg)/day	OVx + PTH
MAR (μm/day)	0.297 ± 0.02***	0.11 ± 0.04	0.291 ± 0.008***	0.294 ± 0.02***	0.276 ± 0.01***	0.37 ± 0.04***
BFR (($\mu m^3/\mu m^2$)/day)	0.27 ± 0.006***	0.10 ± 0.02	0.37 ± 0.006***[b]	0.33 ± 0.005***	0.31 ± 0.014***	0.33 ± 0.015***

[a]Each parameter represents data from 10 mice/group, and values are expressed as the mean ±SEM. (∗∗∗) $p < 0.001$ compared with OVx + vehicle group. [b]Intergroups comparison for compound **18** shows that for 1 (mg/kg)/day dose, $p < 0.001$ when compared with OVx + 10 (mg/kg)/day group, $p < 0.01$ when compared with OVx + 5 (mg/kg)/day group, $p < 0.01$ when compared with OVx + PTH group.

piperidine (0.2 mL) and refluxed. Most of the excess solvent was evaporated under reduced pressure, and the residue was neutralized with acetic acid. To this residue water (25 mL) was added and extracted 3-fold with 20 mL of $CHCl_3$. The combined organic layers were dried on Na_2SO_4, filtered, and concentrated to dryness under reduced pressure.The crude product thus obtained was purified over column chromatography to furnish (0.44 g, 64% yield) compound **5.**

Compounds **6**–**9** were synthesized by above method.

Methyl 8-sec-Butyl-6-formyl-2-oxo-2H-chromene-3-carboxylate (**5**). White solid. Yield 64%. Mp 122–123 °C. IR (KBr): 3062, 1749, 1609, 1576, 1055 cm^{-1}. ^1H NMR ($CDCl_3$, 300 MHz) δ: 10.04 (s, 1H), 8.62 (s, 1H), 8.05 (brs, 1H), 7.98 (brs, 1H), 3.98 (s, 3H), 3.51–3.40 (m, 1H), 1.79–1.69 (m, 2H), 1.32 (d, 3H, J = 7 Hz), 0.88 (t, 3H, J = 7.4 Hz). ^{13}C NMR ($CDCl_3$, 75 MHz) δ: 190.2, 163.4, 156.6, 155.9, 149.0, 137.5, 133.0, 131.9, 129.9, 118.9, 118.1, 53.2, 33.5, 29.7, 20.5, 12.0. ESI-MS m/z: 289 $(M + H)^+$. Anal. Calcd for $C_{16}H_{16}O_5$: C, 66.66; H, 5.59. Found: C, 66.58; H, 5.64.

dx.doi.org/10.1021/jm301281e | J. Med. Chem. 2013, 56, 109–122

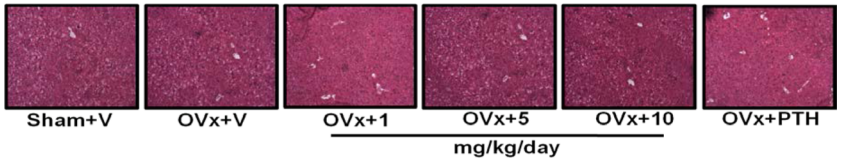

Figure 12. Sections of livers of mice after 2 months of compound **18** treatment. Balb/c mice were administered with tested compound doses (1, 5, 10 (mg/kg)/day) orally.

*Ethyl 8-sec-Butyl-6-formyl-2-oxo-2H-chromene-3-carboxylate (**6**).* White solid. Yield 65%. Mp 89−90 °C. IR (KBr): 3042, 1747, 1601, 1589, 1065 cm^{-1}. ^1H NMR ($CDCl_3$, 300 MHz) δ 10.05 (s, 1H), 8.60 (s, 1H), 8.05(brs, 1H), 8.01 (brs, 1H) 4.44 (q, 2H, J = 7.1 Hz), 3.51−3.40 (m, 1H), 1.78−1.69 (m, 2H), 1.43 (t, 3H, J = 7.1 Hz), 1.33 (d, 3H, J = 7 Hz), 0.88 (t, 3H, J = 7.4 Hz). ^{13}C NMR ($CDCl_3$, 75 MHz) δ: 190.2, 162.7, 156.5, 155.8, 148.5, 137.3, 132.9, 131.7, 129.9, 119.2, 118.0, 62.2, 33.4, 29.6, 20.4, 14.2, 12.0. ESI-MS m/z: 303 $(M + H)^+$. Anal. Calcd for $C_{17}H_{18}O_5$: C, 67.54; H, 6.00. Found: C, 67.59; H, 5.94.

*Methyl 8-tert-Butyl-6-formyl-2-oxo-2H-chromene-3-carboxylate (**7**).* White solid. Yield 68%. Mp 92−93 °C. IR (KBr): 3048, 1741, 1611, 1584, 1061 cm^{-1}. ^1H NMR ($CDCl_3$, 300 MHz) δ: 10.05 (s, 1H), 8.62 (s, 1H), 8.16 (brs, 1H), 8.02 (brs, 1H), 3.98 (s, 3H), 1.55 (brs, 9H). ^{13}C NMR ($CDCl_3$, 75 MHz) δ: 190.2, 163.3, 157.7, 155.3, 149.3, 139.7, 132.5, 131.7, 130.7, 118.6, 118.4, 53.1, 35.4, 29.6. ESI-MS m/z: 289 $(M + H)^+$. Anal. Calcd for $C_{16}H_{16}O_5$: C, 66.66; H, 5.59. Found: C, 66.61; H, 5.62.

*Ethyl 8-tert-Butyl-6-formyl-2-oxo-2H-chromene-3-carboxylate (**8**).* White solid. Yield 71%. Mp 91−92 °C. IR (KBr): 3041, 1746, 1615, 1584, 1066 cm^{-1}. ^1H NMR ($CDCl_3$, 300 MHz) δ: 10.05 (s, 1H), 8.60 (s, 1H), 8.16 (brs, 1H), 8.02 (brs, 1H), 4.43 (q, 2H, J = 7.1 Hz), 1.55 (brs, 9H), 1.42 (t, 3H, J = 7.1 Hz). ^{13}C NMR ($CDCl_3$, 75 MHz) δ: 190.3, 162.7, 157.7, 155.3, 148.8, 139.7, 132.3, 131.6, 130.6, 118.8, 118.6, 62.3, 35.4, 29.6, 14.3. ESI-MS m/z: 303 $(M + H)^+$. Anal. Calcd for $C_{17}H_{18}O_5$: C, 67.54; H, 6.00. Found: C, 67.59; H, 5.96.

General Synthesis of Compounds 9−15. *Dimethyl 4-(8-sec-Butyl-3-(methoxycarbonyl)-2-oxo-2H-chromen-6-yl)-2,6-dimethyl-1,4-dihydropyridine-3,5-dicarboxylate (**11**).* To a solution of ethyl 8-*sec*-butyl-6-formyl-2-oxo-2*H*-chromene-3-carboxylate (1.0 mmol) (**5**) in ethanol were added ethyl acetoacetate (2.0 mmol), ammonium acetate (3.0 mmol), and 3 mL acetic acid. The reaction mixture was continued under reflux condition for 8 h. After completion of reaction (monitored by TLC), the reaction mixture was cooled to room temperature. The solid thus obtained was filtered and chromatographed over EtOAc, furnishing diethyl 4-(8-*sec*-butyl-3-(ethoxycarbonyl)-2-oxo-2*H*-chromen-6-yl)-2,6-dimethyl-1,4-dihydropyridine-3,5-dicarboxylate (**11**) as a white solid.

Compounds **9−15** were prepared in a manner similar to the procedure described above.

*Diethyl 4-(8-sec-Butyl-3-(ethoxycarbonyl)-2-oxo-2H-chromen-6-yl)-2,6-dimethyl-1,4-dihydropyridine-3,5-dicarboxylate (**9**).* White solid. Yield 83%. Mp 240−241 °C. IR (KBr): 3011, 1677, 1591, 1033 cm^{-1}. ^1H NMR ($CDCl_3$, 300 MHz) δ: 8.48 (s, 1H), 7.52 (d, 1H, J = 1.8 Hz), 7.31 (d, 1H, J = 2.0 Hz), 6.09 (s, 1H), 5.04 (s, 1H), 4.40 (q, 2H, J = 7.1 Hz), 4.13−4.06 (m, 4H), 3.34 (q, 1H, J = 7.0 Hz), 2.38 (brs, 6H), 1.69−1.64 (m, 2H), 1.40 (t, 3H, J = 7.1 Hz), 1.26−1.20 (m, 9H), 0.83 (t, 3H, J = 7.2 Hz). ^{13}C NMR ($CDCl_3$, 75 MHz): 167.4, 163.3, 157.3, 155.7, 151.4, 149.9, 144.9, 144.5, 134.4, 132.8, 126.2, 117.6, 116.9, 103.6, 103.5, 61.7, 61.5, 59.8, 39.3, 33.2, 29.6, 22.9, 20.5, 19.4, 14.3, 14.2, 13.8, 11.9. ESI-MS (m/z): 526 $(M + H)^+$. HRMS m/z calcd for $C_{29}H_{35}NO_8$ $(M + H)^+$ 526.2442, found 526.2457. Anal. Calcd for $C_{29}H_{35}NO_8$: C, 66.27; H, 6.71; N, 2.66. Found: C, 66.23; H, 6.77; N, 2.63.

*Dimethyl 4-(8-sec-Butyl-3-(methoxycarbonyl)-2-oxo-2H-chromen-6-yl)-2,6-dimethyl-1,4-dihydropyridine-3,5-dicarboxylate (**10**).* White solid. Yield 87%. Mp 270−271 °C. IR (KBr): 3008, 1684, 1593, 1041 cm^{-1}. ^1H NMR ($CDCl_3$, 300 MHz) δ: 8.52 (s, 1H), 7.52 (d, 1H, J = 1.8 Hz), 7.29 (d, 1H, J = 2.0 Hz), 6.09 (s, 1H), 5.03 (s, 1H), 3.94 (s, 3H), 3.64 (s, 6H), 3.36 (q, 1H, J = 6.6 Hz), 2.38 (brs, 6H), 1.67 (t, 2H, J = 7.1 Hz), 1.25 (d, 3H, J = 6.9 Hz), 0.84 (t, 3H, J = 7.2 Hz). ^{13}C NMR ($CDCl_3$, 75 MHz): 167.9, 164.2, 157.5, 151.7, 150.7, 145.1, 134.7, 133.1, 126.3, 117.9, 116.8, 103.6, 52.9, 51.2, 39.4, 33.2, 29.7, 20.8, 19.6, 11.9. ESI-MS (m/z): 484 $(M + H)^+$. HRMS m/z calcd for $C_{26}H_{29}NO_8$ $(M + H)^+$ 484.1972, found 484.1973. Anal. Calcd for $C_{26}H_{29}NO_8$: C, 64.59; H, 6.05; N, 2.90. Found: C, 64.55; H, 6.01; N, 2.85.

*Diethyl 4-(8-sec-Butyl-3-(methoxycarbonyl)-2-oxo-2H-chromen-6-yl)-2,6-dimethyl-1,4-dihydropyridine-3,5-dicarboxylate (**11**).* White solid. Yield 86%. Mp 245−246 °C. IR (KBr): 3007, 1688, 1588, 1049 cm^{-1}. ^1H NMR ($CDCl_3$, 300 MHz) δ: 8.51 (s, 1H), 7.53 (d, 1H, J = 1.7 Hz), 7.31 (d, 1H, J = 2.1 Hz), 6.16 (s, 1H), 5.05 (s, 1H), 4.13−4.06 (m, 4H), 3.93 (s, 3H), 3.34 (q, 1H, J = 7.0 Hz), 2.37 (brs, 6H), 1.71−1.62 (m, 2H), 1.26−1.19 (m, 9H), 0.83 (t, 3H, J = 7.1 Hz). ^{13}C NMR ($CDCl_3$, 75 MHz): 167.5, 164.2, 157.5, 151.6, 150.7, 145.2, 144.7, 134.6, 133.1, 126.4, 117.8, 116.6, 103.8, 60.0, 52.9, 39.4, 33.3, 29.7, 20.7, 19.7, 14.5, 12.1. ESI-MS (m/z): 512 $(M + H)^+$. HRMS m/z calcd for $C_{28}H_{33}NO_8$ $(M + H)^+$ 512.2285, found 512.2285. Anal. Calcd for $C_{28}H_{33}NO_8$: C, 65.74; H, 6.50; N, 2.74. Found: C, 65.75; H, 6.54; N, 2.71.

*Dimethyl 4-(8-sec-Butyl-3-(ethoxycarbonyl)-2-oxo-2H-chromen-6-yl)-2,6-dimethyl-1,4-dihydropyridine-3,5-dicarboxylate (**12**).* White solid. Yield 81%. Mp 247−248 °C. IR (KBr): 3004, 1680, 1596, 1045 cm^{-1}. ^1H NMR ($CDCl_3$, 300 MHz) δ: 8.48 (s, 1H), 7.51 (d, 1H, J = 1.7 Hz), 7.29 (d, 1H, J = 2.1 Hz), 6.09 (s, 1H), 5.04 (s, 1H), 4.40 (q, 2H, J = 7.1 Hz), 3.64 (brs, 6H), 3.36 (q, 1H, J = 6.8 Hz), 2.38 (s, 6H), 1.67 (t, 2H, J = 7.5 Hz), 1.40 (t, 3H, J = 7.2 Hz), 1.25 (d, 3H, J = 6.9 Hz), 0.83 (t, 3H, J = 7.3 Hz). ^{13}C NMR ($CDCl_3$, 75 MHz): 167.7, 163.3, 157.3, 151.4, 149.9, 144.8, 134.4, 132.7, 125.9, 117.7, 116.9, 103.4, 61.7, 50.9, 39.3, 33.0, 29.5, 20.6, 19.4, 14.2, 11.7. ESI-MS (m/z): 498 $(M + H)^+$. HRMS m/z calcd for $C_{27}H_{31}NO_8$ $(M + H)^+$ 498.2129, found 498.2194. Anal. Calcd for $C_{27}H_{31}NO_8$: C, 65.18; H, 6.28; N, 2.82. Found: C, 65.22; H, 6.25; N, 2.79.

*Dimethyl 4-(8-tert-Butyl-3-(ethoxycarbonyl)-2-oxo-2H-chromen-6-yl)-2,6-dimethyl-1,4-dihydropyridine-3,5-dicarboxylate (**13**).* White solid. Yield 82%. Mp 231−232 °C. IR (KBr): 3005, 1680, 1595, 1048 cm^{-1}. ^1H NMR ($CDCl_3$, 300 MHz) δ: 8.49 (s, 1H), 7.66 (d, 1H, J = 1.9 Hz), 7.30 (d, 1H, J = 1.9 Hz), 6.47 (s, 1H), 5.07 (s, 1H), 4.39 (q, 2H, J = 7.1 Hz), 3.67 (brs, 6H), 2.38 (brs, 6H), 1.46 (s, 9H), 1.40 (t, 3H, J = 7.1 Hz). ^{13}C NMR ($CDCl_3$, 75 MHz): 167.9, 163.5, 156.9, 152.7, 150.4, 145.2, 144.1, 137.4, 132.4, 126.4, 118.2, 116.6, 103.3, 61.9, 51.2, 39.1, 34.9, 29.8, 19.6, 14.4. ESI-MS (m/z): 498 $(M + H)^+$. HRMS m/z calcd for $C_{27}H_{31}NO_8$ $(M + H)^+$ 498.2129, found 498.2145. Anal. Calcd for $C_{27}H_{31}NO_8$: C, 65.18; H, 6.28; N, 2.82. Found: C, 65.25; H, 6.23; N, 2.84.

*Diethyl 4-(8-tert-Butyl-3-(methoxycarbonyl)-2-oxo-2H-chromen-6-yl)-2,6-dimethyl-1,4-dihydropyridine-3,5-dicarboxylate (**14**).* White solid. Yield 85%. Mp 255−256 °C. IR (KBr): 3011, 1681, 1587, 1039 cm^{-1}. ^1H NMR ($CDCl_3$, 300 MHz) δ: 8.51 (s, 1H), 7.64 (d, 1H, J = 1.9 Hz), 7.32 (d, 1H, J = 1.9 Hz), 6.26 (s, 1H), 5.03 (s, 1H), 4.10 (q, 4H, J = 7.1 Hz), 3.93 (s, 3H), 2.37 (s, 6H), 1.47 (s, 9H), 1.22 (t, 6H, J = 7.1 Hz). ^{13}C NMR ($CDCl_3$, 75 MHz): 167.4, 164.2, 156.8, 152.7, 150.8, 144.7, 137.2, 132.8, 126.9, 118.2, 116.3, 103.7, 59.9, 52.8, 39.5, 34.9, 29.9, 19.6, 14.5. ESI-MS (m/z): 512 $(M + H)^+$. HRMS m/z calcd for $C_{28}H_{33}NO_8$ $(M + H)^+$ 512.2285, found 512.2245. Anal. Calcd for $C_{28}H_{33}NO_8$: C, 65.74; H, 6.50; N, 2.74. Found: C, 65.70; H, 6.54; N, 2.71.

*Dimethyl 4-(8-tert-Butyl-3-(methoxycarbonyl)-2-oxo-2H-chromen-6-yl)-2,6-dimethyl-1,4-dihydropyridine-3,5-dicarboxylate (**15**).* White solid. Yield 81%. Mp 248−249 °C. IR (KBr): 3009, 1688, 1597, 1042 cm^{-1}. ^1H NMR ($CDCl_3$, 300 MHz) δ: 8.54 (s, 1H), 7.67 (d, 1H,

dx.doi.org/10.1021/jm301281e | J. Med. Chem. 2013, 56, 109−122

J = 1.9 Hz), 7.31 (d, 1H, J = 1.9 Hz), 6.62 (s, 1H), 5.07 (s, 1H), 3.93 (s, 3H), 3.67 (s, 6H), 2.38 (s, 6H), 1.47 (s, 9H). ^{13}C NMR ($CDCl_3$, 75 MHz): 167.8, 164.1, 152.8, 150.9, 145.2, 144.1, 137.5, 132.6, 126.5, 118.2, 116.2, 103.3, 52.8, 51.2, 39.1, 34.9, 29.9, 19.6. ESI-MS (m/z): 484 $(M + H)^+$. HRMS m/z calcd for $C_{26}H_{29}NO_8$ $(M + H)^+$ 484.1972, found 484.1954. Anal. Calcd for $C_{26}H_{29}NO_8$: C, 64.59; H, 6.05; N, 2.90. Found: C, 64.55; H, 6.07; N, 2.95.

General Synthesis of Compounds 16−29. *(±)-Ethyl 4-(8-sec-Butyl-3-(methoxycarbonyl)-2-oxo-2H-chromen-6-yl)-2,7,7-trimethyl-5-oxo-1,4,5,6,7,8-hexahydroquinoline-3-carboxylate (**18**).* To a solution of methyl 8-*sec*-butyl-6-formyl-2-oxo-2*H*-chromene-3-carboxylate (1.0 mmol) in ethanol were added ethyl acetoacetate (1.0 mmol), dimedone (1.0 mmol), ammonium acetate (3.0 mmol), and 3 mL of acetic acid. The reaction mixture was continued under reflux conditions for 7−8 h. After completion of reaction (monitored by TLC), the reaction mixture was cooled to room temperature. The solid thus obtained was filtered and chromatographed over EtOAc/hexane, providing (±)-ethyl 4-(8-*sec*-butyl-3-(methoxycarbonyl)-2-oxo-2*H*-chromen-6-yl)-2,7,7-trimethyl-5-oxo-1,4,5,6,7,8-hexahydroquinoline-3-carboxylate (**18**) in good yield.

Compounds **16−29** were synthesized in a similar way.

*(±)-Ethyl 4-(8-sec-Butyl-3-(ethoxycarbonyl)-2-oxo-2H-chromen-6-yl)-2-methyl-5-oxo-1,4,5,6,7,8-hexahydroquinoline-3-carboxylate (**16**).* White solid. Yield 89%. Mp 215−216 °C. IR (KBr): 3003, 1681, 1597, 1040 cm^{-1}. ^{1}H NMR ($CDCl_3$, 300 MHz) δ: 8.52 (s, 1H), 7.59 (d, 1H, J = 1.4 Hz), 7.35 (d, 1H, J = 1.9 Hz), 7.27 (s, 1H), 5.15 (s, 1H), 4.41−4.35 (m, 2H), 4.08−4.02 (m, 2H), 3.34−3.25 (m, 1H), 2.51 (s, 2H), 2.41 (s, 3H), 2.34−2.31(m, 3H), 2.03−1.97 (m, 2H), 1.70−1.61 (m, 2H), 1.39 (t, 3H J = 7.1 Hz), 1.25 (t, 3H J = 6.8 Hz), 1.22−1.14 (m, 3H), 0.85−0.79 (m, 3H). ^{13}C NMR ($CDCl_3$, 75 MHz): 195.8, 167.2, 163.1, 157.6, 151.2, 150.2, 144.6, 134.5, 133.2, 126.2, 117.4, 116.5, 112.6, 104.9, 61.7, 59.8, 37.1, 36.3, 33.4, 29.5, 27.2, 21.1, 20.5, 19.1, 14.3, 11.9. ESI-MS (m/z): 508 $(M + H)^+$. HRMS m/z calcd for $C_{29}H_{33}NO_7$ $(M + H)^+$ 508.2336, found 508.2387. Anal. Calcd for $C_{29}H_{33}NO_7$: C, 68.62; H, 6.55; N, 2.76. Found: C, 68.59; H, 6.51; N, 2.71.

*(±)-Methyl 4-(8-sec-Butyl-3-(ethoxycarbonyl)-2-oxo-2H-chromen-6-yl)-2-methyl-5-oxo-1,4,5,6,7,8-hexahydroquinoline-3-carboxylate (**17**).* White solid. Yield 86%. Mp 229−230 °C. IR (KBr): 3005, 1680, 1597, 1046 cm^{-1}. ^{1}H NMR ($CDCl_3$, 300 MHz) δ: 8.52 (s, 1H), 7.58 (s, 1H), 7.34 (d, 1H, J = 1.7 Hz), 7.21 (s, 1H), 5.15 (d, 1H, J = 5.3 Hz), 4.40 (q, 2H, J = 7.1 Hz), 3.60 (s, 3H), 3.30 (p, 1H, J = 6.6 Hz), 2.52 (brs, 2H), 2.40 (s, 3H), 2.34 (s, 2H), 2.04−1.95 (m, 2H), 1.71−1.63 (m, 2H), 1.40 (t, 3H J = 7.1 Hz), 1.23 (t, 3H J = 6.9 Hz), 0.84−0.77 (m, 3H). ^{13}C NMR ($CDCl_3$, 75 MHz): 195.8, 167.7, 163.1, 157.6, 151.3, 150.3, 144.9, 134.6, 133.2, 126.1, 117.5, 116.5, 112.5, 104.7, 61.7, 51.0, 37.0, 36.1, 33.4, 29.4, 27.1, 21.1, 20.4, 19.1, 14.2, 11.8. ESI-MS (m/z): 494 $(M + H)^+$. HRMS m/z calcd for $C_{28}H_{31}NO_7$ $(M + H)^+$ 494.2180, found 494.2191. Anal. Calcd for $C_{28}H_{31}NO_7$: C, 68.14; H, 6.33; N, 2.84. Found: C, 68.12; H, 6.33; N, 2.81.

*(±)-Ethyl 4-(8-sec-Butyl-3-(methoxycarbonyl)-2-oxo-2H-chromen-6-yl)-2-methyl-5-oxo-1,4,5,6,7,8-hexahydroquinoline-3-carboxylate (**18**).* White solid. Yield 85%. Mp 263−264 °C. IR (KBr): 3013, 1679, 1599, 1016 cm^{-1}. ^{1}H NMR ($CDCl_3$, 300 MHz) δ: 8.55 (s, 1H), 7.60 (d, 1H, J = 1.8 Hz), 7.34 (d, 1H, J = 2.1 Hz), 7.04 (s, 1H), 5.15 (s, 1H), 4.09−4.01 (m, 2H), 3.93 (s, 3H), 3.35−3.27 (m, 1H), 2.50 (d, 2H, J = 5.1 Hz), 2.41 (s, 3H), 2.35−2.32 (m, 2H), 2.05−1.88 (m, 2H), 1.68−1.63 (m, 2H), 1.26−1.16 (m, 6H), 0.86−0.79 (m, 3H). ^{13}C NMR ($CDCl_3$, 75 MHz): 195.9, 167.2, 163.8, 157.6, 151.4, 150.8, 144.6, 134.6, 133.5, 126.3, 117.4, 116.2, 112.6, 105.1, 59.9, 52.7, 36.9, 36.3, 33.4, 29.5, 27.2, 21.1, 20.5, 19.1, 14.3, 11.8. ESI-MS (m/z): 494 $(M + H)^+$. HRMS m/z calcd for $C_{28}H_{31}NO_7$ $(M + H)^+$ 494.2180, found 494.2176. Anal. Calcd for $C_{28}H_{31}NO_7$: C, 68.14; H, 6.33; N, 2.84. Found: C, 68.16; H, 6.32; N, 2.83.

*(±)-Methyl 4-(8-sec-Butyl-3-(methoxycarbonyl)-2-oxo-2H-chromen-6-yl)-2-methyl-5-oxo-1,4,5,6,7,8-hexahydroquinoline-3-carboxylate (**19**).* White solid. Yield 85%. Mp 240−241 °C. IR (KBr): 3006, 1694, 1594, 1044 cm^{-1}. ^{1}H NMR ($CDCl_3$, 300 MHz) δ: 8.55 (s, 1H), 7.59 (s, 1H), 7.34 (d, 1H, J = 1.7 Hz), 7.24 (s, 1H), 5.15 (d, 1H, J = 3.7 Hz), 3.92 (s, 3H), 3.60 (s, 3H), 3.35−3.26 (m, 1H), 2.52 (brs, 2H), 2.39−2.34 (m, 5H), 2.03−1.88 (m, 2H), 1.66 (d, 2H, J = 8.3 Hz), 1.25 (d, 3H, J = 6.8 Hz), 0.85−0.79 (m, 3H). ^{13}C NMR ($CDCl_3$, 75 MHz): 195.9, 167.7, 163.7, 157.6, 151.4, 150.9, 144.9, 134.7, 133.4, 126.1, 117.5, 116.1, 112.5, 104.8, 52.7, 51.0, 37.0, 36.2, 33.4, 29.4, 27.1, 21.1, 20.4, 19.1, 11.8. ESI-MS (m/z): 480 $(M + H)^+$. HRMS m/z calcd for $C_{27}H_{29}NO_7$ $(M + H)^+$ 480.2023, found 480.2048. Anal. Calcd for $C_{27}H_{29}NO_7$: C, 67.33; H, 6.10; N, 2.92. Found: C, 67.31; H, 6.14; N, 2.91.

*(±)-Ethyl 4-(8-sec-Butyl-3-(ethoxycarbonyl)-2-oxo-2H-chromen-6-yl)-2,7,7-trimethyl-5-oxo-1,4,5,6,7,8-hexahydroquinoline-3-carboxylate (**20**).* White solid. Yield 88%. Mp 225−226 °C. IR (KBr): 3011, 1686, 1590, 1045 cm^{-1}. ^{1}H NMR ($CDCl_3$, 300 MHz) δ: 8.50 (s, 1H), 7.56 (d, 1H, J = 1.8 Hz), 7.37 (d, 1H, J = 1.8 Hz), 6.75 (s, 1H), 5.13 (s, 1H), 4.39 (q, 2H, J = 7.1 Hz), 4.08−4.04 (m, 2H), 3.30 (p, 1H, J = 6.6 Hz), 2.45 (s, 4H), 2.39−2.10 (m, 3H), 1.67−1.60 (m, 2H), 1.40 (t, 3H, J = 7.1 Hz), 1.25−1.15 (m, 6H), 1.07 (s, 3H), 0.89−0.77 (m, 3H). ^{13}C NMR ($CDCl_3$, 75 MHz): 195.6, 167.2, 163.1, 157.6, 151.3, 150.2, 149.3, 144.8, 134.7, 133.2, 126.2, 117.3, 116.6, 111.3, 105.1, 61.7, 59.9, 50.7, 40.7, 36.4, 33.4, 32.6, 29.7, 26.9, 20.5, 19.2, 14.3, 11.9. ESI-MS (m/z): 536 $(M + H)^+$. HRMS m/z calcd for $C_{31}H_{37}NO_7$ $(M + H)^+$ 536.2649, found 536.2663. Anal. Calcd for $C_{31}H_{37}NO_7$: C, 69.51; H, 6.96; N, 2.62. Found: C, 69.54; H, 6.90; N, 2.55.

*(±)-Methyl 4-(8-sec-Butyl-3-(ethoxycarbonyl)-2-oxo-2H-chromen-6-yl)-2,7,7-trimethyl-5-oxo-1,4,5,6,7,8-hexahydroquinoline-3-carboxylate (**21**).* White solid. Yield 89%. Mp 210−211 °C. IR (KBr): 3010, 1687, 1599, 1046 cm^{-1}. ^{1}H NMR ($CDCl_3$, 300 MHz) δ: 8.51 (s, 1H), 7.56 (d, 1H, J = 1.7 Hz), 7.35 (d, 1H, J = 1.7 Hz), 6.92 (s, 1H), 5.13 (s, 1H), 4.39 (q, 2H, J = 7.1 Hz), 3.61 (s, 3H), 3.35−3.26 (m, 1H), 2.46 (s, 4H), 2.31−2.10 (m, 3H), 1.69−1.61 (m, 2H), 1.42 (t, 3H, J = 7.1 Hz), 1.24−1.21 (m, 3H), 1.07 (s, 1H), 0.89−0.77 (m, 6H). ^{13}C NMR ($CDCl_3$, 75 MHz): 195.7, 167.7, 163.1, 157.7, 151.3, 150.4, 149.2, 145.1, 144.1, 134.8, 133.1, 126.0, 117.3, 116.5, 111.3, 104.7, 61.8, 51.1, 40.7, 36.1, 33.3, 32.9, 29.6, 26.8, 20.6, 19.3, 14.3, 11.9. ESI-MS (m/z): 522 $(M + H)^+$. HRMS m/z calcd for $C_{30}H_{35}NO_7$ $(M + H)^+$ 522.2493, found 522.2470. Anal. Calcd for $C_{30}H_{35}NO_7$: C, 69.08; H, 6.76; N, 2.69. Found: C, 69.02; H, 6.73; N, 2.71.

*(±)-Ethyl 4-(8-sec-Butyl-3-(methoxycarbonyl)-2-oxo-2H-chromen-6-yl)-2,7,7-trimethyl-5-oxo-1,4,5,6,7,8-hexahydroquinoline-3-carboxylate (**22**).* White solid. Yield 90%. Mp 205−206 °C. IR (KBr): 3012, 1688, 1591, 1041 cm^{-1}. ^{1}H NMR ($CDCl_3$, 300 MHz) δ: 8.53 (s, 1H), 7.57 (d, 1H, J = 1.8 Hz), 7.37 (s, 1H), 6.78 (s, 1H), 5.12 (s, 1H), 4.06 (p, 2H, J = 3.1 Hz), 3.93 (s, 3H), 3.33−3.27 (m, 1H), 2.41 (s, 4H), 2.30−2.10 (m, 3H), 1.69−1.60 (m, 2H), 1.25−1.16 (m, 6H), 1.07 (s, 3H), 0.90 (s, 3H), 0.84−0.77 (m, 3H). ^{13}C NMR ($CDCl_3$, 75 MHz): 195.4, 167.1, 163.9, 157.4, 151.4, 150.5, 148.5, 144.2, 134.8, 133.2, 126.2, 117.2, 116.5, 111.6, 105.3, 59.9, 52.7, 50.6, 40.9, 36.3, 33.3, 32.6, 29.5, 26.9, 20.6, 19.3, 14.3, 11.9. ESI-MS (m/z): 522 $(M + H)^+$. HRMS m/z calcd for $C_{30}H_{35}NO_7$ $(M + H)^+$ 522.2493, found 522.2486. Anal. Calcd for $C_{30}H_{35}NO_7$: C, 69.08; H, 6.76; N, 2.69. Found: C, 69.11; H, 6.79; N, 2.66.

*(±)-Methyl 4-(8-tert-Butyl-3-(methoxycarbonyl)-2-oxo-2H-chromen-6-yl)-2-methyl-5-oxo-1,4,5,6,7,8-hexahydroquinoline-3-carboxylate (**23**).* White solid. Yield 85%. Mp 245−246 °C. IR (KBr): 3003, 1681, 1579, 1036 cm^{-1}. ^{1}H NMR ($CDCl_3$, 300 MHz) δ: 8.54 (s, 1H), 7.70 (d, 1H, J = 1.9 Hz), 7.34 (d, 1H, J = 1.8 Hz), 7.21 (s, 1H), 5.17 (s, 1H), 3.93 (s, 3H), 3.64 (s, 3H), 2.53 (t, 2H, J = 7.1 Hz), 2.40−2.33 (m, 5H), 2.05−1.96 (m, 2H), 1.46 (s, 9H). ^{13}C NMR ($CDCl_3$, 75 MHz): 195.9, 167.7, 163.8, 157.0, 152.5, 151.1, 145.0, 143.9, 137.3, 132.9, 126.6, 118.0, 115.7, 112.4, 104.7, 52.7, 51.1, 37.0, 35.9, 34.8, 29.7, 27.2, 21.1, 19.2. ESI-MS (m/z): 478 $(M + H)^+$. HRMS m/z calcd for $C_{27}H_{29}NO_7$ $(M + H)^+$ 480.2023, found 480.2034. Anal. Calcd for $C_{27}H_{29}NO_7$: C, 67.63; H, 6.10; N, 2.92. Found: C, 67.64; H, 6.16; N, 2.96.

*(±)-Ethyl 4-(8-tert-Butyl-3-(methoxycarbonyl)-2-oxo-2H-chromen-6-yl)-2-methyl-5-oxo-1,4,5,6,7,8-hexahydroquinoline-3-carboxylate (**24**).* White solid. Yield 87%. Mp 251−252 °C. IR (KBr): 3005, 1687, 1598, 1044 cm^{-1}. ^{1}H NMR ($CDCl_3$, 300 MHz) δ: 8.54 (s, 1H), 7.71 (d, 1H, J = 1.9 Hz), 7.36 (d, 1H, J = 1.9 Hz), 7.25 (s, 1H), 5.16 (s, 1H), 4.07 (q, 2H, J = 7.1 Hz), 3.93 (s, 3H), 2.55−2.51 (m, 2H), 2.40−2.33 (m, 5H), 2.04−1.95 (m, 2H), 1.47 (s, 9H), 1.18 (t, 3H, J = 7.1 Hz). ^{13}C NMR ($CDCl_3$, 75 MHz): 196.0, 167.3, 163.8,

dx.doi.org/10.1021/jm301281e | J. Med. Chem. 2013, 56, 109−122

157.1, 152.5, 151.0, 144.9, 137.1, 133.2, 126.8, 118.1, 115.7, 112.5, 104.9, 59.9, 52.7, 37.1, 36.3, 34.8, 29.8, 27.2, 21.2, 19.2, 14.4. ESI-MS (m/z): 494 $(M + H)^+$. Anal. Calcd for $C_{28}H_{31}NO_7$: C, 68.14; H, 6.33; N, 2.84. Found: C, 68.17; H, 6.31; N, 2.88.

*(±)-Methyl 4-(8-tert-Butyl-3-(ethoxycarbonyl)-2-oxo-2H-chromen-6-yl)-2-methyl-5-oxo-1,4,5,6,7,8-hexahydroquinoline-3-carboxylate (**25**).* White solid. Yield 88%. Mp 255−256 °C. IR (KBr): 3004, 1683, 1594, 1040 cm^{-1}. ^1H NMR ($CDCl_3$, 300 MHz) δ: 8.51 (s, 1H), 7.69 (d, 1H, J = 1.8 Hz), 7.35 (d, 1H, J = 1.9 Hz), 6.85 (s, 1H), 5.18 (s, 1H), 4.40 (q, 2H, J = 7.1 Hz), 3.64 (s, 3H), 2.53−2.52 (m, 2H), 2.42 (s, 3H), 2.39−2.34 (m, 2H), 2.01−1.91 (m, 2H), 1.47 (s, 9H), 1.41 (t, 3H, J = 7.1 Hz). ^{13}C NMR ($CDCl_3$, 75 MHz): 195.9, 167.7, 163.1, 157.1, 152.4, 151.2, 150.6, 145.2, 143.9, 137.3, 132.8, 126.6, 118.0, 116.0, 112.3, 104.6, 61.7, 51.1, 37.0, 35.9, 34.8, 29.7, 27.1, 21.1, 19.2, 14.3. ESI-MS (m/z): 494 $(M + H)^+$. Anal. Calcd for $C_{28}H_{31}NO_7$: C, 68.14; H, 6.33; N, 2.84. Found: C, 68.11; H, 6.27; N, 2.78.

*(±)-Ethyl 4-(8-tert-Butyl-3-(ethoxycarbonyl)-2-oxo-2H-chromen-6-yl)-2-methyl-5-oxo-1,4,5,6,7,8-hexahydroquinoline-3-carboxylate (**26**).* White solid. Yield 82%. Mp 247−248 °C. IR (KBr): 3005, 1681, 1588, 1037 cm^{-1}. ^1H NMR ($CDCl_3$, 300 MHz) δ: 8.51 (s, 1H), 7.70 (d, 1H, J = 1.8 Hz), 7.36 (d, 1H, J = 1.9 Hz), 7.08 (s, 1H), 5.16 (s, 1H), 4.39 (q, 2H, J = 7.1 Hz), 4.07 (q, 2H, J = 7.1 Hz), 2.52 (t, 2H, J = 6.6 Hz), 2.42 (s, 3H), 2.36−2.34 (m, 2H), 2.05−1.91 (m, 2H), 1.47 (s, 9H), 1.41 (t, 3H, J = 7.1 Hz), 1.18 (t, 3H, J = 7.1 Hz). ^{13}C NMR ($CDCl_3$, 75 MHz): 195.9, 167.3, 163.3, 157.1, 152.5, 150.8, 144.6, 144.1, 137.3, 133.0, 126.8, 118.1, 116.4, 112.7, 105.2, 61.8, 59.8, 59.9, 37.1, 36.4, 34.9, 29.9, 27.4, 21.2, 19.3, 14.4. ESI-MS (m/z): 508 $(M + H)^+$. HRMS m/z calcd for $C_{29}H_{33}NO_7$ $(M + H)^+$ 508.2336, found 508.2338. Anal. Calcd for $C_{29}H_{33}NO_7$: C, 68.62; H, 6.55; N, 2.76. Found: C, 68.55; H, 6.59; N, 2.73.

*(±)-Methyl 4-(8-tert-Butyl-3-(methoxycarbonyl)-2-oxo-2H-chromen-6-yl)-2,7,7-trimethyl-5-oxo-1,4,5,6,7,8-hexahydroquinoline-3-carboxylate (**27**).* White solid. Yield 90%. Mp 231−232 °C. IR (KBr): 3008, 1687, 1588, 1040 cm^{-1}. ^1H NMR ($CDCl_3$, 300 MHz) δ: 8.54 (s, 1H), 7.69 (d, 1H, J = 1.9 Hz), 7.37 (d, 1H, J = 1.8 Hz), 7.16 (s, 1H), 5.13 (s, 1H), 3.93 (s, 3H), 3.64 (s, 3H), 2.48−2.12 (m, 7H), 1.45 (s, 9H), 1.08 (s, 3H), 0.93 (s, 3H). ^{13}C NMR ($CDCl_3$, 75 MHz): 195.7, 167.7, 163.8, 157.1, 152.6, 151.0, 149.5, 145.2, 143.8, 137.6, 132.9, 126.7, 117.9, 115.9, 111.4, 104.9, 52.7, 51.2, 40.9, 36.2, 34.9, 32.8, 29.8, 26.9, 19.3. ESI-MS (m/z): 508 $(M + H)^+$. HRMS m/z calcd for $C_{29}H_{33}NO_7$ $(M + H)^+$ 508.2336, found 508.2311. Anal. Calcd for $C_{29}H_{33}NO_7$: C, 68.62; H, 6.55; N, 2.76. Found: C, 68.66; H, 6.61; N, 2.79.

*(±)-Methyl 4-(8-tert-Butyl-3-(ethoxycarbonyl)-2-oxo-2H-chromen-6-yl)-2,7,7-trimethyl-5-oxo-1,4,5,6,7,8-hexahydroquinoline-3-carboxylate (**28**).* White solid. Yield 89%. Mp 235−236 °C. IR (KBr): 3006, 1685, 1597, 1039 cm^{-1}. ^1H NMR ($CDCl_3$, 300 MHz) δ: 8.51 (s, 1H), 7.67 (d, 1H, J = 1.9 Hz), 7.37 (d, 1H, J = 1.8 Hz), 6.73 (s, 1H), 5.14 (s, 1H), 4.40 (q, 2H, J = 7.1 Hz), 3.64 (s, 3H), 2.42 (s, 3H), 2.32−2.13 (m, 3H), 1.45−1.39 (m, 12H), 1.09 (s, 3H), 0.93 (s, 3H). ^{13}C NMR ($CDCl_3$, 75 MHz): 195.7, 167.8, 163.2, 157.1, 152.5, 150.6, 149.5, 145.2, 143.8, 137.5, 132.7, 126.6, 117.9, 116.3, 111.4, 104.8, 61.7, 51.1, 40.8, 36.2, 34.9, 32.7, 29.8, 26.9, 19.3, 14.4. ESI-MS (m/z): 522 $(M + H)^+$. HRMS m/z calcd for $C_{30}H_{35}NO_7$ $(M + H)^+$ 522.2493, found 522.2431. Anal. Calcd for $C_{30}H_{35}NO_7$: C, 69.08; H, 6.76; N, 2.69. Found: C, 69.12; H, 6.71; N, 2.73.

*(±)-Ethyl 4-(8-tert-Butyl-3-(ethoxycarbonyl)-2-oxo-2H-chromen-6-yl)-2,7,7-trimethyl-5-oxo-1,4,5,6,7,8-hexahydroquinoline-3-carboxylate (**29**).* White solid. Yield 87%. Mp 234−235 °C. IR (KBr): 3007, 1686, 1595, 1040 cm^{-1}. ^1H NMR ($CDCl_3$, 300 MHz) δ: 8.51 (s, 1H), 7.69 (d, 1H, J = 1.8 Hz), 7.39 (d, 1H, J = 1.7 Hz), 7.04 (s, 1H), 5.12 (s, 1H), 4.40 (q, 2H, J = 7.1 Hz), 4.08 (q, 2H, J = 7.1 Hz), 2.41−2.05 (m, 7H), 1.45 (s, 9H), 1.41 (t, 3H, J = 7.1 Hz), 1.20 (t, 3H, J = 7.1 Hz), 1.08 (s, 3H), 0.92 (s, 3H). ^{13}C NMR ($CDCl_3$, 75 MHz): 195.6, 167.3, 163.3, 157.1, 152.5, 150.5, 149.3, 144.8, 144.0, 137.4, 132.9, 126.9, 117.9, 116.4, 111.5, 105.2, 61.8, 60.0, 50.8, 40.9, 36.5, 34.9, 32.8, 29.9, 27.0, 19.3, 14.4. ESI-MS (m/z): 536 $(M + H)^+$. HRMS m/z calcd for $C_{31}H_{37}NO_7$ $(M + H)^+$ 536.2649, found 536.2658. Anal. Calcd for $C_{31}H_{37}NO_7$: C, 69.51; H, 6.96; N, 2.62. Found: C, 69.56; H, 6.88; N, 2.67.

Biological Methods. Cytotoxicity Assay. The toxicity of synthesized compounds was tested on calvarial osteoblast cells. Cells were cultured in the absence or presence of compounds at various concentrations (1 pM to 1 μM) for 48 h. The cell viability was determined by using MTT (3-(4, 5-dimethylthiazol-2-yl)-2,5-diphenyltetrazolium bromide) assay.[16]

Culture of Calvarial Osteoblasts. For each experiment, about 25−30 calvaria were harvested from 1−2 day old mice pups (both sexes). Briefly, an individual calvarium was surgically isolated from the skull. Sutures were segregated, and adherent tissue material was cleaned by gentle scrapping. Isolated calvaria were pooled and kept for repeated digestion (15 min/digestion) with 0.1% dispase, and 0.1% collagenase P was used to release cells. The supernatant of the first digestion was discarded. Cells from the next three digestions were pooled and cultured in α modified essential medium (α-MEM) containing 10% fetal calf serum (FCS) and 1% penicillin/streptomycin (complete growth medium). For experiments 70−80% confluent mice calvarial osteoblasts were used.[23]

Alkaline Phosphatase Assay. At 70−80% confluency mice calvarial osteoblasts were trypsinized, and 2×10^3 cells/well were seeded onto 96-well plates for alkaline phosphatase (ALP) measurement. Cells were treated with different concentrations of test compound or vehicle for 48 h in α-MEM supplemented with 10% charcoal treated FCS, 10 mM β-glycerophosphate, 50 μg/mL ascorbic acid, and 1% penicillin/streptomycin (osteoblast differentiation medium). At the end of the incubation period, the total ALP activity was measured using p-nitrophenyl phosphate (PNPP) as substrate and absorbance was read at 405 nm.[24,25]

Mineralized Nodule Formation Assay. Mice calvarial osteoblast was seeded onto 12-well plates (10 000 cells/well) in osteoblast differentiation medium. Mice calvarial osteoblasts were cultured with or without test compounds for 21 days, and after every 48 h media were changed. At the end of the experiment, cells were washed with phosphate-buffered saline (PBS) and fixed with 4% paraformaldehyde in PBS for 15 min. The fixed cells were stained with alizarin red-S (40 mM, pH 4.5) for 30 min followed by washing with tap water. Stained cells were first photographed under a light microscope, and alizarin stain was then extracted by using 10% (v/v) acetic acid with shaking at room temperature for 30 min. Cells were scrapped out from wells and centrifuged (20000g for 15 min), and the supernatant was collected. To the supernatant, 10% (v/v) ammonium hydroxide was added to bring the pH of the solution to 4.5 for color formation. Absorbance of the solution was read at 405 nm.[26]

In Vivo Experiments. The study was conducted in accordance with current legislation on animal experiments [Institutional Animal Ethical Committee (IAEC) at CDRI]. Eight-week old adult female Balb/c mice were used for the study. Animals were housed at 21 °C in 12 h light/12 h dark cycles. Normal chow diet and water were provided ad libitum. Ten mice/group were taken for the study. The animals were ovariectomized and left for 8 weeks for osteopenia to develop. Thereafter, the animals were divided into groups as follows: sham (ovary intact) + vehicle (gum acacia in distilled water), OVx + vehicle, OVx + 1.0, 5.0, and 10.0 (mg/kg)/day body weight dose of compound **18** and standard control group OVx + PTH. Mice were treated with compound **18** or vehicle once daily for 8 weeks by oral gavage. After the period of 8 weeks, animals were sacrificed and femur bones were collected for analysis of trabecular microarchitecture. μCT experiments were carried out using Sky Scan 1076 micro-CT scanner (Aartselaar, Belgium) as previously reported.[27] For ex vivo experiments bone marrow from the femur of the vehicle and compound **18** treated mice was flushed and cultured in osteoblast differentiation medium (10 nM dexamethasone, 10 mM β-glycerophosphate, and 50 μg/mL ascorbic acid) for 18 days. Alizarin red-S stain was used for staining mineralized nodules followed by extraction of the stain for quantitation.[23]

Analysis of Bone Turnover Markers.[28,29] Serum samples separated after autopsy were used for the experiment. On the basis of our previously published protocols, serum osteocalcin (mid-portion) were determined by enzyme-linked immunosorbent assay

kits by following the manufacturer's protocols (Immunodiagnostic Systems Inc.).[15]

Quantitative Real-Time Polymerase Chain Reaction (qPCR). qPCR reaction was performed for quantitative comparative measurement of the expression of osteoblast specific genes Runx-2, ALP, ColI, BMP-2, and OCN following an optimized protocol described before.[28] The housekeeping gene GAPDH was used as the internal control in this study. Primers were designed using the Universal Probe Library (Roche Applied Sciences) for the selected genes.[28] For real-time PCR, cDNA was synthesized with Revert Aid cDNA synthesis kit (Fermentas, Austin, TX, U.S.) using 2.0 μg of total RNA. SYBR green chemistry was used to perform quantitative determination of relative expression of transcripts for all genes. All genes were analyzed using the Light Cycler 480 (Roche Molecular Biochemicals, Indianapolis, IN, U.S.) real time PCR machine.

Fluorochrome Labeling and Bone Histomorphometry. For determination of new-bone formation in vivo, each mouse received intraperitoneal administration of fluorochromes tetracycline (20 mg/kg) on days 40 and 68 and calcein (20 mg/kg) on days 4 and 54, following a previously published protocol.[23] At autopsy, femur bone was dissected out and (50 μm thickness) cross sections were cut using an Isomet slow speed bone cutter (Buehler, Lake Bluff, IL, U.S.). Photographs of the sections were taken under a fluorescent microscope aided with appropriate filters. Histomorphometric analysis for bone formation, such as for the determination of mineral appositional rate (MAR) and bone formation rate (BFR), was performed using Leica-Qwin software (Leica Microsystems Inc., Buffalo Grove, IL, U.S.) as described in our previously published protocol.[25]

In Vivo Toxicity and Liver Histology. Following treatment with compound **18**, livers from different groups were harvested and fixed in 4% formaldehyde. A sample of each liver was dehydrated in ascending grades of isopropanol, cleared in xylene, and embedded in paraffin wax using standard procedures. Transverse sections (5 μm) were stained with Erhlichs hematoxylin and eosin, and representative images were captured using a Leica Qwin camera.

Western Blot Analysis. Mouse calvarial osteoblasts were grown 60−70% confluence followed by treatment with nifedipine and compounds **10**, **14**, **18**, **22** for 48 h. The cells were washed with cold phosphate buffered saline (PBS), and whole cell lysates were prepared by the addition of lysis buffer, Sigma Aldrich (St. Louis, MO, U.S.), containing a protease inhibitor mixture, Sigma Aldrich (St. Louis, MO, U.S.). Aliquots of 20−40 μg of cell lysates were separated on SDS−PAGE under reducing conditions (Bio-Rad, Hercules, CA, U.S.) and then transferred to polyvinylidene difluoride (PVDF) membranes (Millipore, Watford, U.K.). Membrane was blocked for nonspecific binding in 5% nonfat dry milk and followed by incubation with an primary antibody (Abcam, Cambridge, U.S.) at 4 °C overnight. Membranes were washed and were probed with a horseradish peroxidase conjugated secondary antibody (Abcam, Cambridge, U.S.). Western blot signals were detected and visualized by an enhanced chemiluminescence system (GE Healthcare Life Sciences, India).[23]

■ ASSOCIATED CONTENT

Ⓢ Supporting Information

Detailed spectral analysis (1D and 2D NMR) for all the new compounds, together with X-ray crystallographic details for compound **15**. This material is available free of charge via the Internet at http://pubs.acs.org.

■ AUTHOR INFORMATION

Corresponding Author

*For K.V.S.: phone, +91 9919317940; fax, +91-518-2623405; e-mail, sashidhar123@gmail.com and kv_sashidhara@cdri.res.in. For R.T.: phone, +91 9415769219; e-mail, ritu_pgi@yahoo.com and ritu_trivedi@cdri.res.in.

Author Contributions

‖These authors contributed equally.

Notes

The authors declare no competing financial interest.

■ ACKNOWLEDGMENTS

Instrumentation facilities from SAIF, CDRI are gratefully acknowledged. M.K., R.K.M., and A. K. are thankful to CSIR, New Delhi, India, for financial support. Generous funding from the Ministry of Health and Family Welfare (Grant-in-Aid), Government of India, is acknowledged. The authors are grateful to the Director, CDRI, Lucknow, India, for constant encouragement in the drug development program. This is CSIR-CDRI Communication No. 8367.

■ ABBREVIATIONS USED

ALP, alkaline phosphatase; BFR, bone formation rate; BMP-2, bone morphogenic protein 2; ER, estrogen receptor; GAPDH, glyceraldehydes 3-phosphate dehydrogenase; IAEC, Institutional Animal Ethics Committee; MAR, mineral appositional rate; MOB, mouse calvarial osteoblast; OVx, ovariectomized; PTH, parathyroid hormone; qPCR, quantitative real-time polymerase chain reaction; RANKL, receptor activator of nuclear factor κB ligand; RUNX2, runt-related transcription factor 2; μCT, microcomputed tomography

■ ADDITIONAL NOTE

This manuscript is part 26 in the series "Advances in Drug Design and Discovery" CSIR-CDRI #8367.

■ REFERENCES

(1) Riggs, B. L.; Parfitt, A. M. Drugs used to treat osteoporosis: the critical need for a uniform nomenclature based on their action on bone remodeling. *J. Bone Miner. Res.* **2005**, *20*, 177−184.

(2) Ershler, W. B. New concepts in the pathogenesis and treatment of osteoporosis. *Front. Biomed.* **2000**, *1*, 41−51.

(3) Kyoko, T.; Shinji, F.; Takaya, I.; Kazutoshi, N.; Satoshi, K.; Koichiro, T. Incadronate inhibits osteoporosis in ovariectomized rats. *Eur. J. Pharmacol.* **2002**, *457*, 51−56.

(4) (a) Sekiya, I.; Larson, B. L.; Vuoristo, J. T.; Cui, J. G.; Prockop, D. J. Adipogenic differentiation of human adult stem cells from bone marrow stroma (MSCs). *J. Bone Miner. Res.* **2004**, *19*, 256−264. (b) Verma, S.; Rajaratnam, J. H.; Denton, J.; Hoyland, J. A.; Byers, R. J. Adipocytic proportion of bone marrow is inversely related to bone formation in osteoporosis. *J. Clin. Pathol.* **2002**, *55*, 693−698. (c) Burkhardt, R.; Kettner, G.; Bohm, W.; Schmidmeier, M.; Schlag, R.; Frisch, B.; Mallmann, B.; Eisenmenger, W.; Gilg, T. Changes in trabecular bone, hematopoiesis and bone marrow vessels in aplastic anemia, primary osteoporosis, and old age: a comparative histomorphometric study. *Bone* **1987**, *8*, 157−164.

(5) (a) Sato, M.; Grese, T. A.; Dodge, J. A.; Bryant, H. U.; Turner, C. H. Emerging therapies for the prevention or treatment of postmenopausal osteoporosis. *J. Med. Chem.* **1999**, *42*, 1−24. (b) Ebina, K.; Fukuhara, A.; Shimomura, I. Role of adipocytokine in bone metabolism. *Clin. Calcium* **2008**, *18*, 623−630.

(6) (a) Strazzullo, P.; Nunziata, V.; Cirillo, M.; Giannattasio, R.; Ferrara, L. A.; Mattioli, P. L.; Mancini, M. Abnormalities of calcium metabolism in essential hypertension. *Clin. Sci.* **1983**, *65*, 137−141. (b) McCarron, D. A.; Pingree, P. A.; Rubin, R. J.; Gaucher, S. M.; Molitch, M.; Krutzik, S. Enhanced parathyroid function in essential hypertension: a homeostatic response to a urinary calcium leak. *Hypertension* **1980**, *2*, 162−168.

(7) Tsuda, K.; Nishio, I.; Masuyama, Y. Bone mineral density in women with essential hypertension. *Am. J. Hypertens.* **2001**, *14*, 704−707.

(8) Halici, Z.; Borekci, B.; Ozdemir, Y.; Cadirci, E.; Suleyman, H. Protective effects of amlodipine and lacidipine on ovariectomy-induced bone loss in rats. *Eur. J. Pharmacol.* **2008**, *579*, 241−245.
(9) Ushijima, K.; Liu, Y.; Maekawa, T.; Ishikawa, E.; Motosugi, Y.; Ando, H.; Tsuruoka, S.; Fujimura, A. Protective effect of amlodipine against osteoporosis in stroke-prone spontaneously hypertensive rats. *Eur. J. Pharmacol.* **2010**, *635*, 187−230.
(10) (a) Kennedy, R. O.; Thornes, R. D. *Coumarins Biology, Applications and Mode of Action*; Wiley: New York, 1997. (b) Hoult, J. R.; Paya, M. Pharmacological and biochemical actions of simple coumarins: natural products with therapeutic potential. *Gen. Pharmacol.* **1996**, *27*, 713−722.
(11) (a) Li, X. X.; Hara, I.; Matsumiya, T. Effects of osthole on postmenopausal osteoporosis using ovariectomized rats. Comparison to the effects of estradiol. *Biol. Pharm. Bull.* **2002**, *25*, 738−742. (b) Tang, C. H.; Yang, R. S.; Chien, M. Y.; Chen, C. C.; Fu, W. M. Enhancement of bone morphogenetic protein-2 expression and bone formation by coumarin derivatives via p38 and ERK-dependent pathway in osteoblasts. *Eur. J. Pharmacol.* **2008**, *579*, 40−49. (c) Tang, D. Z.; Yang, F.; Yang, Z.; Huang, J.; Shi, Q.; Chen, D.; Wang, Y. J. Psoralen stimulates osteoblast differentiation through activation of BMP signalling. *Biochem. Biophys. Res. Commun.* **2011**, *405*, 256−261. (d) Ming, L. G.; Zhou, J.; Cheng, G. Z.; Ma, H. P.; Chen, K. M. Osthole, a coumarin isolated from common Cnidium fruit, enhances the differentiation and maturation of osteoblasts in vitro. *Pharmacology* **2011**, *88*, 33−44.
(12) (a) Sashidhara, K. V.; Kumar, A.; Kumar, M.; Singh, S.; Jain, M.; Dikshit, M. Synthesis of novel 3-carboxamide-benzocoumarin derivatives as orally active antithrombotic agents. *Bioorg. Med. Chem. Lett.* **2011**, *21*, 7034−7040. (b) Sashidhara, K. V.; Kumar, M.; Modukuri, R. K.; Srivastava, A.; Puri, A. Discovery and synthesis of novel substituted benzocoumarins as orally active lipid modulating agents. *Bioorg. Med. Chem. Lett.* **2011**, *21*, 6709−6713. (c) Sashidhara, K. V.; Kumar, A.; Chatterjee, M.; Rao, K. B.; Singh, S.; Verma, A. K.; Palit, G. Discovery and synthesis of novel 3-phenylcoumarin derivatives as antidepressant agents. *Bioorg. Med. Chem. Lett.* **2011**, *21*, 1937−1941. (d) Sashidhara, K. V.; Kumar, A.; Kumar, M.; Sonkar, R.; Bhatia, G.; Khanna, A. K. Novel coumarin derivatives as potential antidyslipidemic agents. *Bioorg. Med. Chem. Lett.* **2010**, *20*, 4248−4251. (e) Sashidhara, K. V.; Rosaiah, J. N.; Kumar, A.; Bhatia, G.; Khanna, A. K. Synthesis of novel benzocoumarin derivatives as lipid lowering agents. *Bioorg. Med. Chem. Lett.* **2010**, *20*, 3065−3069. (f) Sashidhara, K. V.; Kumar, A.; Kumar, M.; Srivastava, A.; Puri, A. Synthesis and antihyperlipidemic activity of novel coumarin bisindole derivatives. *Bioorg. Med. Chem. Lett.* **2010**, *20*, 6504−6507. (g) Sashidhara, K. V.; Rosaiah, J. N.; Kumar, Gara, R. K.; Nayak, L. V.; Srivastava, K.; Bid, H. K.; Konwar, R. Neo-tanshinlactone inspired synthesis, in vitro evaluation of novel substituted benzocoumarin derivatives as potent anti-breast cancer agents. *Bioorg. Med. Chem. Lett.* **2010**, *20*, 7127−7131.
(13) Sashidhara, K. V.; Kumar, A.; Kumar, M.; Sarkar, J.; Sinha, S. Synthesis and in vitro evaluation of novel coumarin-chalcone hybrids as potential anticancer agents. *Bioorg. Med. Chem. Lett.* **2010**, *20*, 7205−7211.
(14) Hantzsch, A. Condensationprodukteaus aldehydammoniak und ketoniartigen verbindungen. *Chem. Ber.* **1881**, *14*, 1637−1638.
(15) Trivedi, R.; Kumar, S.; Kumar, A.; Siddiqui, J. A.; Swarnkar, G.; Gupta, V.; Kendurker, A.; Dwivedi, A. K.; Romero, J. R.; Chattopadhyay, N. Kaempferol has osteogenic effect in ovariectomized adult Sprague-Dawley rats. *Mol. Cell. Endocrinol.* **2008**, *289*, 85−93.
(16) Sharma, A.; Chakravarti, B.; Gupt, M. P.; Siddiqui, J. A.; Konwar, R.; Tripathi, R. P. Synthesis and anti breast cancer activity of biphenyl based chalcones. *Bioorg. Med. Chem.* **2010**, *18*, 4711−4720.
(17) Manferdini, C.; Gabusi, E.; Grassi, F.; Piacentini, A.; Cattini, L.; Zini, N.; Filardo, G.; Facchini, A.; Lisignoli, G. Evidence of specific characteristics and osteogenic potentiality in bone cells from tibia. *J. Cell. Physiol.* **2011**, *226*, 2675−2682.
(18) Bhargavan, B.; Gautam, A. K.; Singh, D.; Kumar, A.; Chaurasia, S.; Tyagi, A. M.; Yadav, D. K.; Mishra, J. S.; Singh, A. B.; Sanyal, S.; Goel, A.; Maurya, R.; Chattopadhyay, N. Methoxylated isoflavones, cajanin and isoformononetin, have non-estrogenic bone forming effect via differential mitogen activated protein kinase (MAPK) signaling. *J. Cell. Biochem.* **2009**, *108*, 388−399.
(19) Trivedi, R.; Kumar, A.; Gupta, V.; Kumar, S.; Nagar, G. K.; Romero, J. R.; Dwivedi, A. K.; Chattopadhyay, N. Effects of Egb 761 on bone mineral density, bone microstructure, and osteoblast function: possible roles of quercetin and kaempferol. *Mol. Cell. Endocrinol.* **2009**, *302*, 86−91.
(20) Verdelis, K.; Lukashova, L.; Atti, E.; Mayer-Kuckuk, P.; Peterson, M. G.; Tetradis, S.; Boskey, A. L.; Van der Meulen, M. C. MicroCT morphometry analysis of mouse cancellous bone: intra- and inter-system reproducibility. *Bone* **2011**, *49*, 580−587.
(21) Turner, C. H. Determinants of skeletal fragility and bone quality. *J. Musculoskeletal Neuronal Interact.* **2002**, *2*, 527−528.
(22) Turner, C. H. Biomechanics of bone: determinants of skeletal fragility and bone quality. *Osteoporosis Int.* **2002**, *13*, 97−104.
(23) Sharan, K.; Mishra, J. S.; Swarnkar, G.; Siddiqui, J. A.; Khan, K.; Kumari, R.; Rawat, P.; Maurya, R.; Sanyal, S.; Chattopadhyay, N. A novel quercetin analogue from a medicinal plant promotes peak bone mass achievement and bone healing after injury and exerts an anabolic effect on osteoporotic bone: the role of aryl hydrocarbon receptor as a mediator of osteogenic action. *J. Bone Miner. Res.* **2011**, *26*, 2096−2111.
(24) Dixit, P.; Chillara, R.; Khedgikar, V.; Gautam, J.; Kushwaha, P.; Kumar, A.; Singh, D.; Trivedi, R.; Maurya, R. Constituents of *Dalbergia sissoo* Roxb. leaves with osteogenic activity. *Bioorg. Med. Chem. Lett.* **2012**, *22*, 890−897.
(25) Siddiqui, J. A.; Swarnkar, G.; Sharan, K.; Chakravarti, B.; Gautam, A. K.; Rawat, P.; Kumar, M.; Gupta, V.; Manickavasagam, L.; Dwivedi, A. K.; Maurya, R.; Chattopadhyay, N. A naturally occurring rare analog of quercetin promotes peak bone mass achievement and exerts anabolic effect on osteoporotic bone. *Osteoporosis Int.* **2011**, *22*, 3013−3027.
(26) Gregory, C. A.; Gunn, W. G.; Peister, A.; Prockop, D. J. An alizarin red-based assay of mineralization by adherent cells in culture: comparison with cetylpyridinium chloride extraction. *Anal. Biochem.* **2004**, *329*, 77−84.
(27) Hildebrand, T.; Ruegsegger, P. Quantification of bone microarchitecture with the structure model index. *Comput. Methods Biomech. Biomed. Engin.* **1997**, *1*, 15−23.
(28) Swarnkar, G.; Sharan, K.; Siddiqui, J. A.; Mishra, J. S.; Khan, K.; Khan, M. P.; Gupta, V.; Rawat, P.; Maurya, R.; Dwivedi, A. K.; Sanyal, S.; Chattopadhyay, N. A naturally occurring naringenin derivative exerts potent bone anabolic effects by mimicking oestrogen action on osteoblasts. *Br. J. Pharmacol.* **2012**, *165*, 1526−1542.
(29) Gautam, J.; Kushwaha, P.; Swarnkar, G.; Khedgikar, V.; Nagar, G. K.; Singh, D.; Singh, V.; Jain, M.; Barthwal, M.; Trivedi, R. EGb 761 promotes osteoblastogenesis, lowers bone marrow adipogenesis and atherosclerotic plaque formation. *Phytomedicine* **2012**, *19*, 1134−1142.
(30) Khedgikar, V.; Gautam, J.; Kushwaha, P.; Kumar, A.; Nagar, G. K.; Dixit, P.; Chillara, R.; Voruganti, S.; Singh, S. P.; Uddin, W.; Jain, G. K.; Singh, D.; Maurya, R.; Chattopadhyay, N.; Trivedi, R. A standardized phytopreparation from an Indian medicinal plant (*Dalbergia sissoo*) has antiresorptive and bone-forming effects on a postmenopausal osteoporosis model of rat. *Menopause* **2012**, *19*, 1336−1346.
(31) Kumar, A.; Gupta, G. K.; Khedgikar, V.; Gautam, J.; Kushwaha, P.; Changkija, B.; Nagar, G. K.; Gupta, V.; Verma, A.; Dwivedi, A. K.; Chattopadhyay, N.; Mishra, P. R.; Trivedi, R. In vivo efficacy studies of layer-by-layer nano-matrix bearing kaempferol for the conditions of osteoporosis: a study in ovariectomized rat model. *Eur. J. Pharm. Biopharm.* **2012**, *82*, 508−517.

■ NOTE ADDED AFTER ASAP PUBLICATION

After this paper was published online December 18, 2012, a correction was made to Figure 7. The correction version was reposted December 24, 2012.